



Mapping Nitrogen Deposition 2015 for Switzerland

Technical Report on the Update of Critical Loads and Exceedance, including the years 1990, 2000, 2005 and 2010

Commissioned by: Federal Office for the Environment (FOEN)

Imprint

Commissioned by	Federal Office for the Environment FOEN Air Pollution Control and Chemicals Division CH-3003 Bern
	The FOEN is an agency of the Federal Department of the Environment, Transport, Energy and Communications (DETEC).
Contractor	Meteotest AG, Fabrikstrasse 14, CH-3012 Bern
Authors	Beat Rihm, Thomas Künzle
FOEN support	Reto Meier
Note	This report was prepared under contract to the Federal Office for the Environment (FOEN). The contractor bears sole responsibility for the content.

Bern, 29.01.2019

Summary

This report presents methods, input data and results related to critical loads for nitrogen (CLN), atmospheric nitrogen deposition and the resulting exceedances of CLN for the year 2015. It is an update of the report by Rihm & Achermann 2016 and it shows mainly the revised data, working steps and results. Depositions and exceedances for the years 1990, 2000, 2005 and 2010 were also recalculated as far as improved data and methods were available.

Acknowledgements

The update of the report on critical loads of nitrogen approach in Switzerland was requested and financed by the Swiss Federal Office for the Environment (FOEN), Air Pollution Control and Chemicals Division. First, I would like to thank Reto Meier (FOEN) for his support, which was highly competent and very helpful. I would also like to thank Eva Seitler (FUB), Thomas Kupper (HAFL) as well as Constantin Streit and Mathias Kuhn (Federal Office for Agriculture) and the Federal Statistical Office for providing valuable data and information.

Beat Rihm, January 2019

Contents

1	Introduction	7
2	Critical Loads of Nutrient Nitrogen	8
3	Mapping Nitrogen Deposition	10
3.1	Modelling Approach	10
3.2	Wet Deposition	10
3.3	Dry Deposition of Gases and Aerosols.....	13
3.4	Mapping Ammonia	13
3.4.1	Emissions of Ammonia	13
3.4.2	Ammonia Concentration	27
3.5	Updates of the Maps 1990, 2000, 2005 and 2010.....	34
4	Results	36
4.1	Critical Loads of Nitrogen.....	36
4.2	Deposition of Nitrogen	37
4.3	Exceedances of Critical Loads of Nitrogen.....	39
A	References	43
B	Annex: Time series maps	46

Tables

Table 1:	Swiss ammonia emissions for different source categories in 2015 ¹ ..	14
Table 2:	Emission factors, number of animals and total NH ₃ -emissions for the 24 animal categories in 2015.....	17
Table 3:	Transfers of nitrogen between biogas/composting facilities and agriculture (farms) for different products in 2015 (FOAG 2017a). Units: kg total N (N _{ges}). The highlighted transfers are related to emissions of manure application on farms (see text).....	20
Table 4:	Total deposition of N compounds in Switzerland 2015.	38
Table 5:	Total deposition of N compounds in Switzerland; years 1990–2015. Units: kt N a ⁻¹	39
Table 6:	Exceedance of critical loads (percent of the ecosystem area) on the 1x1 km ² raster.	41
Table 7:	Exceedance of critical loads of nutrient nitrogen for different protected ecosystems in Switzerland. Units: percent of total ecosystem area.	42

Figures

Figure 1:	Illustration of the method used to convert the original inventory data for raised bogs (polygons, blue colour) to a ha-raster (pink colour). ...	8
-----------	--	---

Figure 2:	Precipitation, average 2013–2017, 1 x 1 km ² raster.	11
Figure 3:	Concentration in rainwater of ammonium (above) and nitrate (below), average 2013–2017, 1 x 1 km ² raster.	12
Figure 4:	NO ₂ concentration, annual mean 2014–2016, 200x200 m ² raster. ...	13
Figure 5:	Ammonia emissions 2015, modelled on 100 x 100 m ² raster.	15
Figure 6:	Transportations of manure defined by linking the zip-codes of the sender and the receiver in 2015. The map shows North-eastern Switzerland. Large clusters can indicate major biogas/composting facilities or companies involved in manure transport.	19
Figure 7:	Net nitrogen fluxes per zip-code caused by manure transports in 2015 (data source FOAG 2017a). Negative values indicate net export (blue-green colours), positive values mean net import (orange-red colours).	21
Figure 8:	Reductions and additions of ammonia emissions from manure application caused by manure transports according to the HODUFLU database 2015 (FOAG 2017a).	22
Figure 9:	The emissions of summered animals are subtracted from the yearly emissions on each farm sending animals. The map shows these emission reductions; for better display a GIS-density function (radius 2 km) was applied.	23
Figure 10:	Carrying capacity of the summering farms (alps) provided by FOAG (2017b). The number of LSU per site were transformed to LSU/ha by a GIS-density function with radius 2 km. Blue lines: cantonal borders.	24
Figure 11:	(1) Weight of farms sending the summering livestock calculated from the respective ammonia emissions by a density function with radius 8 km. (2) Ammonia emissions from alpine agricultural areas due to summering. (3) Blue lines: cantonal borders.	25
Figure 12:	Non-agricultural ammonia emission 2015 modelled on a ha-raster. .	27
Figure 13:	NH ₃ concentration as a function of the distance to a source emitting 1 kg NH ₃ a ⁻¹ for distances between 50 m and 50 km (by Asman & Jaarsveld 1990).	29
Figure 14:	Schematic distance-functions. Left: rotation-symmetric use of p(D) in the Alps. Right: modified p(D, R) function according to prevailing wind directions in the Jura/Plateau region.	29
Figure 15:	The twelve wind regions used for the local dispersion modelling (0–4 km distance from sources) with their prevailing wind direction.	30
Figure 16:	The four wind regions used for the regional dispersion modelling (4–50 km distance from sources).	31
Figure 17:	Relative elevation Hrel2 (elevation minus minimum elevation within a radius of 2 km).	32
Figure 18:	Relationship between the residuals (ratio modelled to measured ammonia concentrations) and the relative elevation (Hrel2).	32

Figure 19: Map of NH ₃ concentration in 2015 (100 x 100 m ² raster) and monitoring sites.	33
Figure 20: Comparison of measured and modelled ammonia concentrations (µg m ⁻³), n=148 (blue markers). The monitoring sites with distances <150 m to farms or obviously incorrect farm coordinates were not included into the regression (red markers).	34
Figure 21: Revised map of the empirical critical loads (CL _{emp} (N)) in Switzerland.	36
Figure 22: Revised map of combined critical loads calculated as minimum of CL _{emp} (N) and CL _{nut} (N) per km ²	37
Figure 22: Total deposition of nitrogen calculated on a 1 x 1 km ² raster.	38
Figure 23: Total nitrogen deposition 1990–2015 in Switzerland calculated by EMEP (EMEP 2018, Gauss et al. 2016) and by the national model (KMBAS).	39
Figure 24: Exceedance of critical loads for (semi-)natural ecosystems (CL _{emp} (N)) by nitrogen depositions in 2015.	40
Figure 25: Exceedance of critical loads for productive forests (CL _{nut} (N)) by nitrogen depositions in 2015. Forest grid: WSL 1990/92.	40
Figure 26: Combined map showing the maximum exceedance of critical loads for forests (CL _{nut} (N)) and (semi-)natural ecosystems (CL _{emp} (N)) by nitrogen depositions in 2015 per 1 x 1 km ² raster cell.	41
Figure 27: Cumulative frequency distribution of the exceedances of critical loads of nutrient nitrogen for different protected ecosystems. Units: percent of total ecosystem area. Nitrogen deposition: year 2015.	42

1 Introduction

The report on critical loads of nitrogen (N) and their exceedances in Switzerland by Rihm & Achermann (2016) showed data and results for the years 1990, 2000 and 2010. The objective of this study was the update of those maps for the year 2015. In addition, some improvements and recalculations were also made for the years 1990, 2000 and 2010. For creating the map of 2015, the following data and methods were updated:

- Ammonia emissions from agriculture: Livestock data of 2015 (SFSSO 2017) and corresponding stratified emission factors for the animal categories (Bonjour & Kupper 2017) were used.
- Spatial allocation of ammonia emissions from manure application: The regional transport of manure was included based on new data from the HODUFLU-database (FOAG 2017a).
- Spatial allocation of ammonia emissions from summering of cattle on alpine pastures: New data on the location of summering farms were included (FOAG 2017b).
- Ammonia dispersion model: The statistical dispersion functions were adapted to different orientations of alpine valleys and regions. The model output was calibrated with monitoring results (Seitler 2018).
- Wet deposition: Precipitation maps (MeteoSwiss 2018) and wet-only measurements (NABEL 2018) were used for the period 2013-2017. For Southern Switzerland, Steingruber (2018) provided results of regression analysis that were used to map N concentrations in precipitation.
- Updated versions of national nature reserves were used for mapping empirical critical loads ($CL_{emp}(N)$): raised bogs (HM), fens (FM) and dry grasslands (TWW) were revised in November 2017. The methods for estimating the critical loads for poor and rich fens was slightly adjusted according to the availability of data.

2 Critical Loads of Nutrient Nitrogen

Critical loads of nutrient nitrogen for productive forest ecosystems ($CL_{nut}(N)$) calculated with the Simple Mass Balance method (Rihm and Achermann 2016, chapter 2.3) were not changed.

Empirical critical loads ($CL_{emp}(N)$) were remapped based on the most recent versions of the Federal Inventory of Raised and Transitional Bogs (HM) of National Importance, the Federal Inventory of Fenlands (FM) of National Importance and the Federal Inventory of Dry Grasslands (TWW) of National Importance.

The three inventories can be downloaded¹ as vector-data (polygons). They were converted to a ha-raster by selecting each cell covered, at least partially, by a protection area, as shown in Figure 1. The ha-raster was used for producing spatially aggregated maps that could be combined with other critical load data on the 1x1 km² raster (Vegetation atlas by Hegg et al. 2003, National Forest Inventory NFI). The ha-raster was also used for calculating exceedance maps.

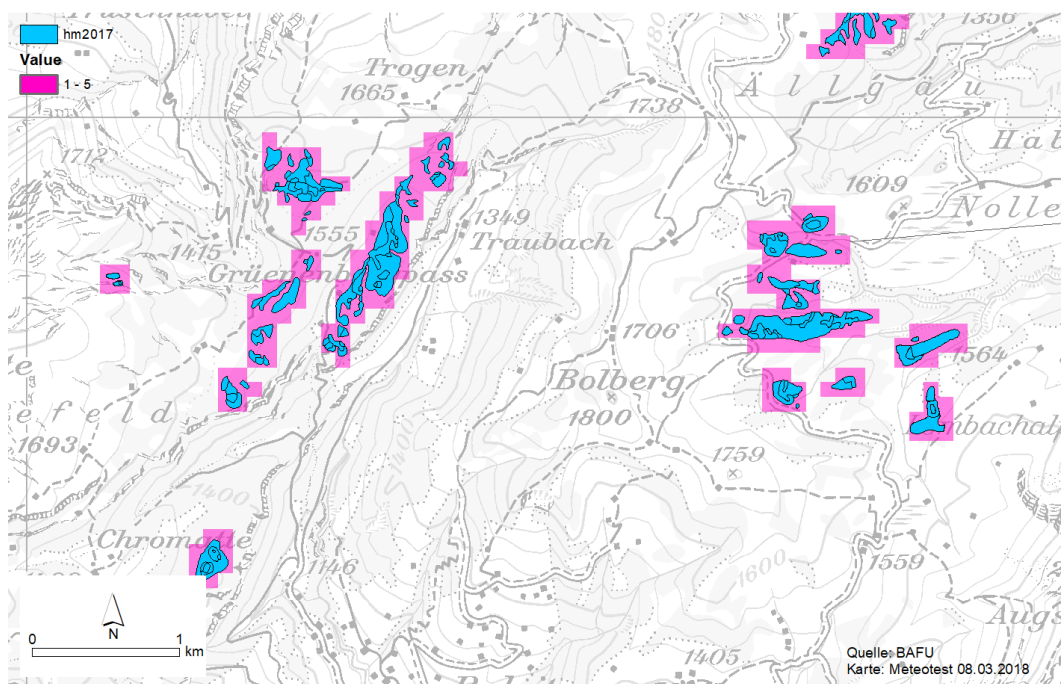


Figure 1: Illustration of the method used to convert the original inventory data for raised bogs (polygons, blue colour) to a ha-raster (pink colour).

The critical loads for fens were slightly adapted to the vegetation data available for the updated Federal Inventory of Fenlands (FM) of National Importance. Only the national protection areas were included, i.e. fens of regional importance were

¹ <https://www.bafu.admin.ch/bafu/en/home/state/data/geodata/biodiversity--geodata.html> [21.08.2018]

not considered. The critical loads for fens were determined using additional information (Hunziker 2018) on vegetation groups occurring on the individual areas. The following criteria were applied:

- If *Scheuchzerietalia* or typical vegetation of raised bogs occur the ecosystem type is defined as 'poor fens' with $CL_{emp}(N) = 10 \text{ kg N ha}^{-1} \text{ a}^{-1}$, else
- if *Caricion fuscae* occurs the ecosystem type is defined as 'poor fens' with $CL_{emp}(N) = 12 \text{ kg N ha}^{-1} \text{ a}^{-1}$, else
- if *Caricion davallianae* or *Molinion* occur the ecosystem type is defined as 'rich fens' with $CL_{emp}(N) = 15 \text{ kg N ha}^{-1} \text{ a}^{-1}$, else
- the remaining FM-areas with occurrence of *Phragmition*, *Magnocaricion* or *Calthion/Filipendulion* were mapped as 'rich fens', with $CL_{emp}(N) = 20 \text{ kg N ha}^{-1} \text{ a}^{-1}$.

The empirical critical loads for raised bogs, dry grasslands, selected ecosystem types from Hegg et al. (1993), hay meadows from the Swiss Biodiversity Monitoring Network and the sensitive alpine lakes were not changed.

3 Mapping Nitrogen Deposition

3.1 Modelling Approach

The general approach for modelling and mapping nitrogen deposition was adopted from Rihm & Achermann (2016). Maps of emissions, concentrations and depositions were calculated for the years 1990, 2000, 2005, 2010 and newly 2015. The year 2007 was not mapped any more, instead the year 2005 was chosen.

For 2000, 2005 and 2010 identical methods were used, i.e. it is a homogenous time series. For the year 1990, a somewhat modified method adapted to the availability of ammonia emission data was applied. For the year 2015, additional data and refined methods were used for mapping emissions and concentrations of ammonia.

The following chapters present the approach and input data used for the year 2015 insofar they differ from the Report 2016.

3.2 Wet Deposition

Wet deposition was obtained by multiplying the annual precipitation rate with mean concentrations of soluble inorganic N compounds in precipitation. For precipitation and concentrations, a 5-year-average (2013–2017) was used. Maps with interpolated precipitation amounts were supplied by MeteoSwiss (2018, see Figure 2). In regions with high precipitation, the calculated deposition can be overestimated as the scavenging effect (wash-out of gases and particles by rain) gets smaller. Therefore, precipitation was limited to maximum of 1'800 mm a⁻¹ in the deposition computation.

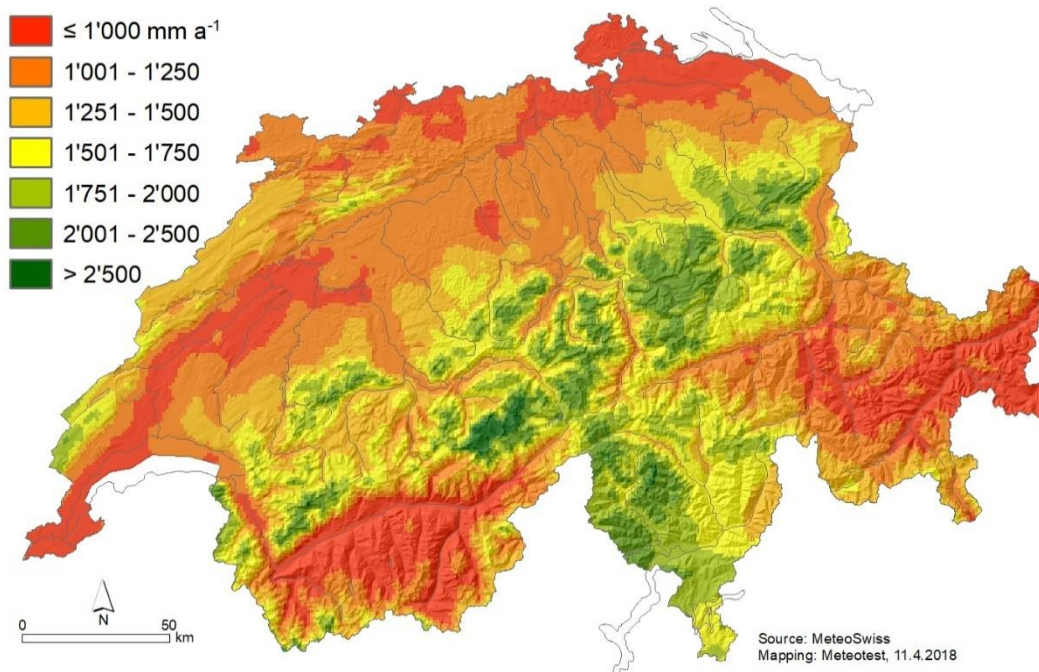


Figure 2: Precipitation, average 2013–2017, 1 x 1 km² raster.

For mapping concentrations of ammonia (NH₄⁺) and nitrate (NO₃⁻) in rain water, different approaches are used in Northern and Southern Switzerland.

In Northern Switzerland (including Alps), data of the National Air Pollution Monitoring Network (NABEL 2018) on wet deposition imply that the concentrations are highest in Central Switzerland (monitoring station Dübendorf) and that they are lower in the Western part of Switzerland (station Payerne). Therefore, the concentrations of Dübendorf and Payerne were interpolated along the west-east axis for altitudes below 800 m. At higher altitudes the concentrations are lower as can be seen in the differences between Payerne (489 m) and Chaumont (1136 m) as well as between Dübendorf (432 m) and Rigi (1031 m). Additional data from bulk measurements made at higher altitudes (Seitler et al. 2016) indicate a clear decrease in concentration above 800 m. Based on this information we roughly assumed a linear decrease of 80% between 800 and 2'500 m altitude and again a constant concentration above 2'500 m.

In Southern Switzerland, the wet-only monitoring network is relatively dense. Besides the NABEL site at Magadino, the Canton Ticino also measures wet deposition at several sites at different altitudes. Concentrations in rain water and deposition maps were calculated by regression models considering longitude, latitude and altitude. They were initially developed by Barbieri & Pozzi (2001) and updated most recently by Steingruber 2018a. For the period 2013–2017, ammonium and nitrate concentrations in precipitation can be calculated for the region of the Canton Ticino as follows (Steingruber 2018b):

$$C_{\text{wet}}(\text{NH}_4^+) = 31.06 + 0.00004695 \cdot x - 0.0002386 \cdot y - 0.005747 \cdot z$$

$$C_{\text{wet}}(\text{NO}_3^-) = 3.09 + 0.00005418 \cdot x - 0.0001259 \cdot y - 0.003069 \cdot z$$

where:

$C_{\text{wet}}(\text{N})$ = concentration of N-compound in rain water [meq m^{-3}]
 x, y = longitude/latitude in Swiss projection LV03² (m)
 z = altitude (m)

The resulting rainwater concentration maps are shown in Figure 3.

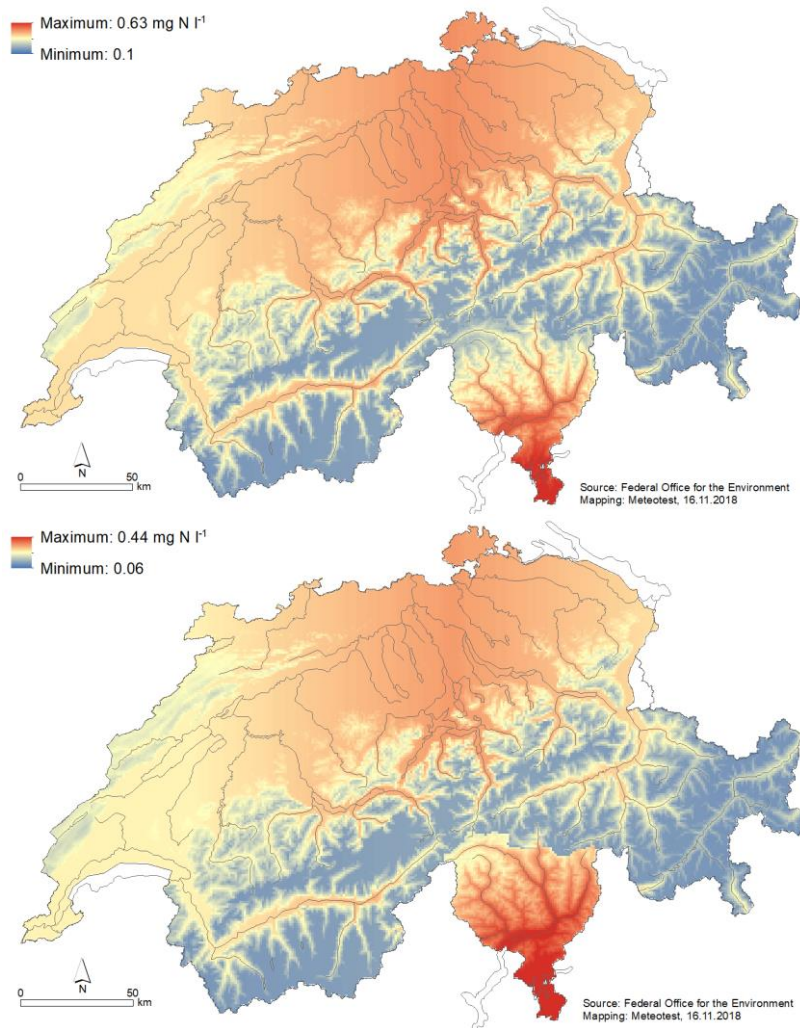


Figure 3: Concentration in rainwater of ammonium (above) and nitrate (below), average 2013–2017, 1 x 1 km² raster.

² <http://www.swisstopo.admin.ch/internet/swisstopo/en/home/topics/survey/sys/refsys/projections.html>

3.3 Dry Deposition of Gases and Aerosols

In general, the methods and data for mapping dry deposition were the same as used by Rihm & Achermann (2016). The maps for HNO₃ and aerosols as well as the deposition velocities for all compounds were not changed.

For NO₂, annual concentration maps from 1990 to 2016 were available on a 200x200 m² raster from the Federal Office for the Environment (BAFU, 2017). For calculating gaseous deposition for the reference year 2015, the 3-year-mean 2014–2016 of NO₂ concentration was used (Figure 4), as for calculating critical load exceedances averaged depositions are preferred to values of single years.

The modelling of ammonia emissions and concentrations was improved (see chapter 3.4).

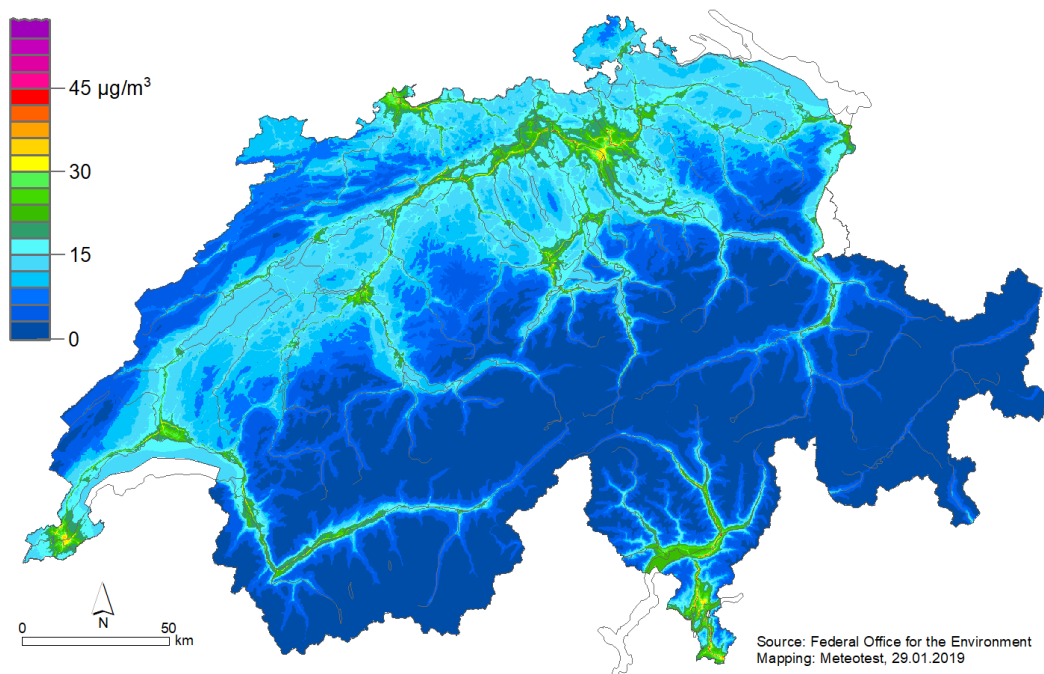


Figure 4: NO₂ concentration, annual mean 2014–2016, 200x200 m² raster.

3.4 Mapping Ammonia

3.4.1 Emissions of Ammonia

a) Overview

The emissions of ammonia in 2015 were modelled based on new livestock statistics (SFSO 2017), the national inventory of air pollutants (FOEN 2017) and new model results for emissions from road transportation (INFRAS 2017). Foreign

emissions within a distance of 50 km to the Swiss border were taken from the ED-GAR dataset (JRC 2017), which has a resolution of approximately 7 by 10 km².

Table 1 shows a summary of the total emissions in Switzerland: agriculture is the main source of NH₃ accounting for about 92% of total ammonia emissions, other anthropogenic sources account for 7% and natural sources for 1%.

The emission maps were calculated with a resolution of 100x100 m². Figure 5 shows the map of total NH₃ emissions in 2015. The following sections show the mapping methods in more detail.

Table 1: Swiss ammonia emissions for different source categories in 2015¹.

Source category	Emission	
	(kt NH ₃ -N a ⁻¹)	Percent
Housing/hardstandings	14.61	29.5%
Storage of manure	6.83	13.8%
Application of manure	18.41	37.1%
Grazing	1.08	2.2%
Total livestock	40.93	82.5%
Mineral fertilizers	1.82	3.7%
Organic recycling fertilizers	0.58	1.2%
Cropland, grassland, alpine pastures	2.34	4.7%
Total plant production	4.73	9.5%
Total agriculture	45.66	92.1%
Commerce and industry	0.46	0.9%
Transport	1.47	3.0%
Households	0.85	1.7%
Waste treatment	0.55	1.1%
Total non-agriculture	3.34	6.7%
Natural sources	0.60	1.2%
Total emission	49.60	100.0%

¹ The emission data presented here is slightly higher than the more recent data reported in Kupper et al. (2018). The deviation is due to recent changes in the Agrammon model since November 2017. This difference does not affect the subsequently modelled ambient NH₃-concentrations as the concentrations are calibrated with measured NH₃-concentrations (see chapter 3.4.2).

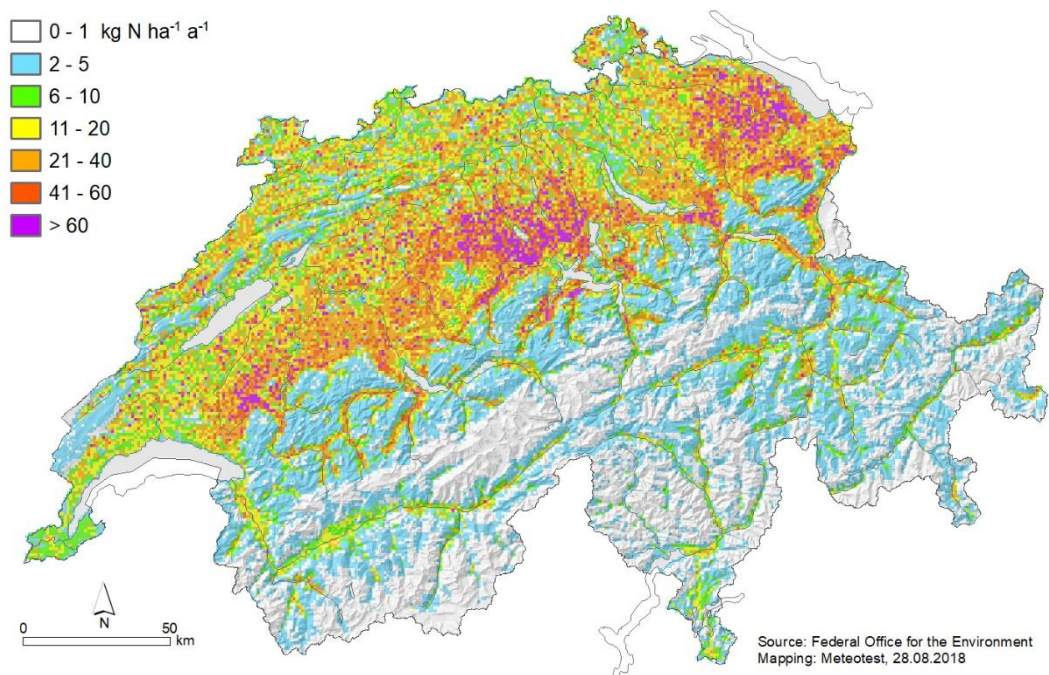


Figure 5: Ammonia emissions 2015, modelled on 100 x 100 m² raster.

b) Emissions from livestock/animal production

The emissions from animal husbandry were modelled with livestock statistics of the year 2015 (SFSO 2017) using a 'bottom-up' approach (i.e. with georeferenced activity data and emission factors). The emissions from traffic were also modelled 'bottom-up'. The other emission categories (crop farming, industries, households, waste treatment and natural sources) were spatially allocated in a top-down approach to the relevant categories of a land-use map. The procedure is summarised in the following sections.

The SFSO (2017) supplied the livestock per farm (codes x1110 to x1890) as well the locations of 53'232 farms (coordinates rounded to hectometres). In 2015, there were 45'383 farms reporting livestock data. Hence, the emissions from animal husbandry were calculated for each of these farm (f) as:

$$E(f)_s = \sum_a (N(f)_a \cdot EF_{acs}) \quad (\text{equation 3.1})$$

where:

$E(f)_s$	=	NH ₃ -emissions on the farm f at the emission stage s [kg NH ₃ -N a ⁻¹].
s	=	emission stage (housing, manure storage, manure application, grazing)
$N(f)_a$	=	number of animals in category a on the farm f.
a	=	animal category (see Table 2).

- EF_{acs} = emission factor of animal category a in farm class c at the emission stage s [$\text{kg NH}_3\text{-N a}^{-1} \text{ animal}^{-1}$].
- c = farm class; combines geographic region, altitude zone and production type.

For each farm, the livestock numbers were multiplied with emission factors that are stratified into 24 animal categories, 6 emission stages and 32 farm classes ('Schichten'). The fully stratified emission factors (not shown) were calculated and supplied by Bonjour & Kupper (2017). Farm classes account for the differences in production techniques in various regions of the country, also reflecting the implementation of emission reduction measures. It is derived by combining three geographic regions (Central, Eastern and Western/Southern Switzerland), three altitude zones (valley, hill and mountain) and five production types (arable farms, cattle farms, pig/poultry farms, mixed farms and other farms) as shown by Kupper et al. (2018).

Table 2 presents an overview of the total animal numbers in Switzerland, the mean emission factors (emission per animal) for four emission stages (housing/hardstandings, storage of liquid and solid manure, application of liquid and solid manure, grazing) and the resulting total emissions from animal husbandry. The mean emission factors per animal and stage were calculated by dividing the total emission of all farms by the total number of animals.

The total emission in Switzerland from animal production amounts to 40.93 kt $\text{NH}_3\text{-N}$. This is 3% more than the results given by Kupper et al. (2018) for the year 2015. The difference is due to recent changes in the Agrammon model since November 2017.

Table 2: Emission factors, number of animals and total NH₃-emissions for the 24 animal categories in 2015.

Code	2015 Animal category	Emission factor (kg NH ₃ -N/a per animal)					Total	Number of animals	Emission (kt NH ₃ -N/a)
		Housing, hard standings	Storage manure	Application manure	Grazing				
DC	Dairy cows	10.10	6.02	17.87	0.82	34.82	583'277	20.31	
H1	Dairy followers <1 year	2.70	1.55	3.44	0.24	7.93	226'519	1.80	
H2	Dairy followers 1–2 years	3.50	1.96	4.75	0.63	10.85	212'845	2.31	
H3	Dairy followers >2 years	5.27	2.69	7.64	0.64	16.23	109'526	1.78	
SC	Suckling cows	8.64	4.59	10.27	1.22	24.72	117'895	2.91	
CS	Pre beef-fattening calves	2.22	1.26	2.45	0.33	6.26	82'276	0.51	
BC	Beef cattle	4.80	2.32	6.28	0.08	13.48	138'321	1.86	
FC	Beef calves	2.08	1.44	3.14	0.01	6.67	83'647	0.56	
PD	Dry sows	7.38	1.08	2.88	0.00	11.33	93'348	1.06	
PN	Farrowing sows	8.26	2.01	6.36	0.00	16.62	29'432	0.49	
PP	Piglets <25 kg	0.69	0.17	0.58	0.00	1.44	329'976	0.48	
PE	Boars	5.04	0.67	2.18	0.01	7.90	2'682	0.02	
PF	Fattening pigs	2.87	0.48	1.47	0.00	4.83	777'256	3.75	
PG	Poultry growers	0.04	0.02	0.03	0.00	0.09	1'032'974	0.10	
PL	Laying hens	0.11	0.04	0.09	0.02	0.26	2'821'943	0.74	
PB	Broilers	0.04	0.01	0.04	0.00	0.09	6'897'769	0.65	
PT	Turkeys	0.20	0.06	0.14	0.02	0.42	49'307	0.02	
PO	Other poultry	0.08	0.05	0.05	0.01	0.19	22'623	0.00	
HU	Horses >3 years	4.64	2.70	2.98	0.41	10.73	50'798	0.55	
HL	Horses <3 years	4.17	2.37	2.25	0.61	9.40	4'681	0.04	
OA	Ponies, donkeys, mules	1.65	0.97	1.00	0.18	3.79	19'682	0.07	
OS	Sheep	1.22	0.78	0.83	0.25	3.08	203'995	0.63	
OM	Milk sheep	1.72	0.90	0.81	0.41	3.84	13'564	0.05	
OG	Goats	1.77	1.05	1.21	0.10	4.13	56'121	0.23	
	Total							40.93	

For spatial attribution of emissions, it was assumed that the emissions from housing, hard standings and manure storage are located in the same hectare-cell as the farm buildings (total 21.4 kt NH₃-N a⁻¹, see Table 1). The emissions from manure application and grazing (total 18.4 and 1.1 kt NH₃-N a⁻¹, respectively, see Table 1) were distributed over the agricultural areas within the corresponding municipalities.

Municipality boundaries (status 2006) were used as a proxy for the land managed by the farms as it is not known, on a national level, which parcels belong to a specific farm. The municipality areas are available in digital form at swisstopo (2006). The size of the 2'827 municipalities varies from about 3 km² in the Plateau to more than 100 km² in alpine regions (average 14 km²). Inside each municipality, the land use-map (SFSO 2013, nomenclature NOAS04) with a resolution

of one hectare and 72 categories was used to enhance the accuracy of the spatial emission pattern. For the emissions from manure application, this was done by weighting the land-use categories as follows (land-use code in parenthesis):

- Weight = 1: orchards (37), horticulture (40), arable land (41), meadows (42) and farm pastures (43).
- Weight = 0.25: vineyards (39), brush meadows/farm pastures (44), open forest on agricultural areas (55) and (if not in summering zone) alpine meadows (45) and favourable alpine pastures (46). These categories are assumed to emit much less ammonia than arable land and regular meadows because fertilization is less intense.

For the emissions from grazing the following weighting was used:

- Weight = 1: Field fruit trees (38), meadows (42), farm pastures (43)
- Weight = 0.25: Brush meadows/farm pastures (44), favourable alpine pastures (46), open forest on agricultural areas (55).

All other land-use categories were excluded from the area sources. Furthermore, all areas protected by the Federal Inventories of Raised and Transitional Bogs, of Fenland and of Dry Grassland (see Chapter 2) were excluded as fertilizing is generally not allowed.

c) Accounting for manure transport (HODUFLU)

Swiss farmers are obligated to register each transport of manure from and to their farm in a central database named HODUFLU (*Hofdüngerflüsse*). The database is hosted by the Federal Office for Agriculture (FOAG)³. Besides manure, it includes also transport of recycling fertilizers as well as transport to biogas or composting facilities. Obviously, this translocation of manure influences the spatial distribution of ammonia emissions from manure application. Therefore, the registered shipments of the year 2015 were used to account for this effect in the emission map.

FOAG (2017a) provided anonymized records of manure transports in 2015, including a total of 46'000 shipments containing 17.4 kt N. Spatial evaluation of the transport routes were inferred based on the zip-codes of the sender and the recipient (Figure 6). Coordinates and GIS-data of the zip-codes are supplied by the Geodesy and Federal Directorate of Cadastral Surveying⁴.

³ <https://www.blw.admin.ch/blw/de/home/politik/datenmanagement/agate/hoduflu.html>

⁴ <https://www.cadastre.ch/en/services/service/plz.html>

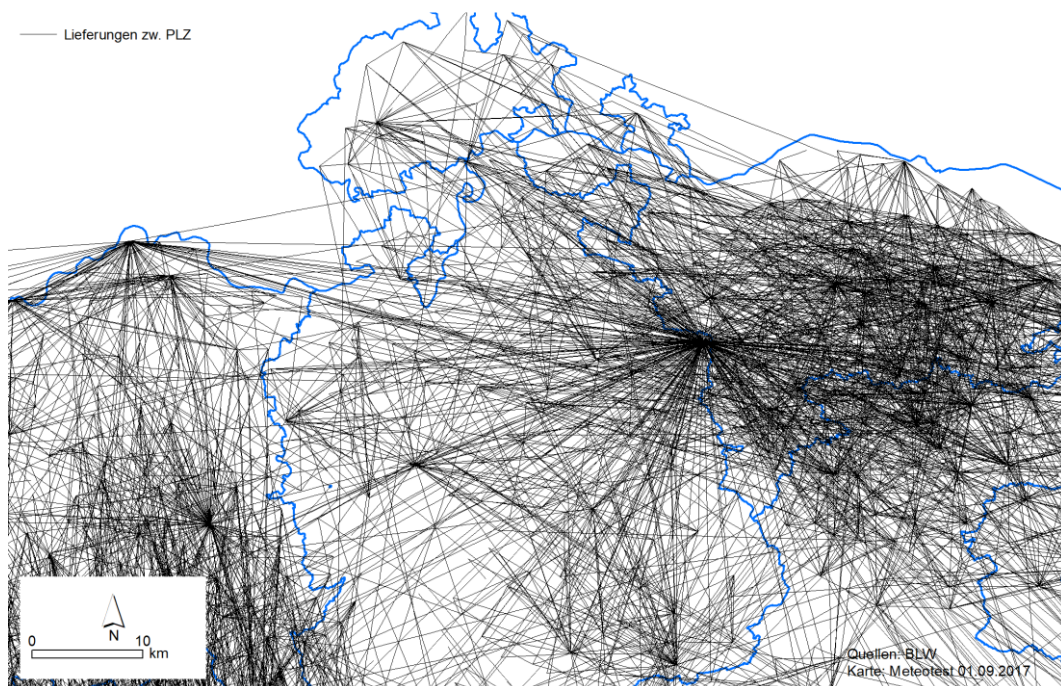


Figure 6: Transportations of manure defined by linking the zip-codes of the sender and the receiver in 2015. The map shows North-eastern Switzerland. Large clusters can indicate major biogas/composting facilities or companies involved in manure transport.

In addition to the zip-codes and the amount of total N (N_{ges}), the transportation receipts indicate the type of sender, the type of receiver and the product specification. The types of sender/receiver are: biogas facilities, composting facilities and farms. With this information, the deliveries that are relevant for the ammonia emissions can be extracted and their net balance for each zip-code can be calculated. Table 3 shows a summary of the nitrogen amounts transferred between the different sender/receiver types and the product categories in 2015 (FOAG 2017a). The following transfers are relevant for the emissions from manure application:

- Deliveries from farms to biogas/composting (all products) cause lower emissions at the sending farms (highlighted in green, Table 3).
- Deliveries from farms to farms (all products) cause lower emissions at the sender and higher emissions at the receiver (highlighted in purple, Table 3).
- Deliveries of some selected products from biogas or composting facilities to farms cause higher emissions at the receiving farms (highlighted in red, Table 3).

The sum of the relevant fluxes is 14.0 kt N. Based on present data manure and recycling fertilizers cannot be strictly separated if biogas or composting facilities are involved in the transfers. The chosen procedure attempts to identify the nitrogen fluxes in form of solid and liquid manure as accurate as possible.

Table 3: Transfers of nitrogen between biogas/composting facilities and agriculture (farms) for different products in 2015 (FOAG 2017a). Units: kg total N (N_{ges}). The highlighted transfers are related to emissions of manure application on farms (see text).

Type of sender	Type of receiver			Total
	Biogas	Compost	Farm	
Biogas	352'158	22'669	3'962'973	4'337'799
solid digestate	138'690		481'056	619'745
liquid digestate	102'185	9'353	2'215'241	2'326'778
thin liquid manure	27'560		416'050	443'610
liquid manure	72'931	958	519'665	593'554
unspecified digestate	1'399		266'451	267'850
solid manure	9'394	12'358	64'511	86'262
Compost	10'627	64'707	1'944'224	2'019'558
Farm	1'930'663	329'363	8'796'861	11'056'887
Total	2'293'448	416'739	14'704'058	17'414'245

By summing up all relevant transports, the net balance of the fluxes can be calculated per zip-code. Figure 7 shows a map of the net nitrogen fluxes per zip-code area. 29% of the transports were made within the same zip-code and were therefore not considered.

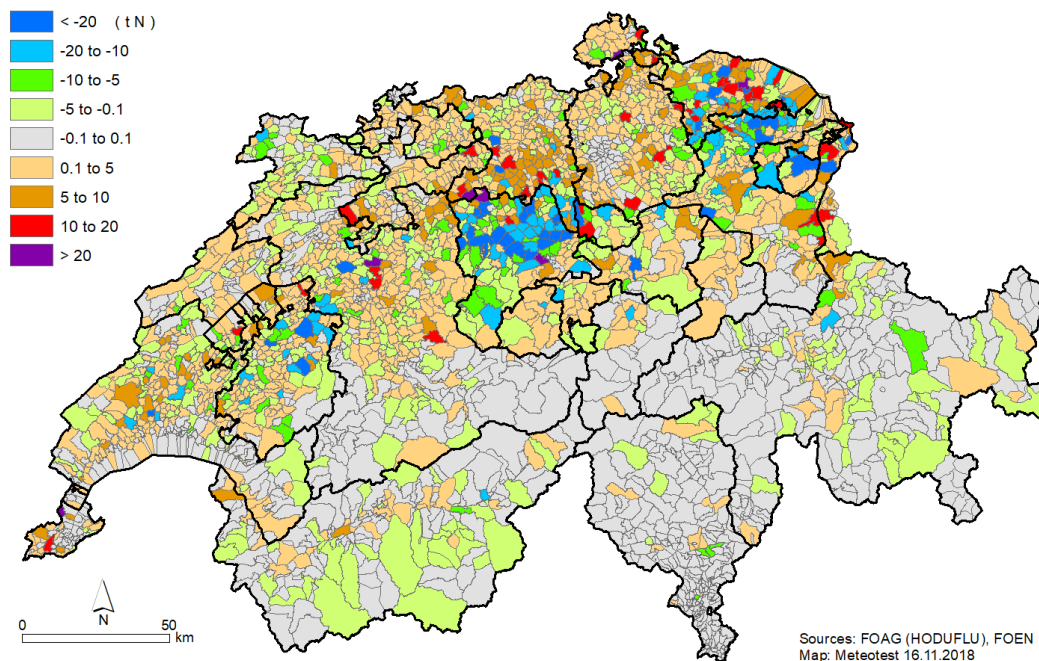


Figure 7: Net nitrogen fluxes per zip-code caused by manure transports in 2015 (data source FOAG 2017a). Negative values indicate net export (blue-green colours), positive values mean net import (orange-red colours).

There are several zip-code areas with very high exports or imports (see Figure 7) that can be explained by large biogas/composting facilities or transportation companies located at these sites. Such highly frequented nodes can also be seen in Figure 6. It can be assumed that those high net fluxes are not related directly to manure application but are rather due to effects of the high storage capacities at those facilities such as inter-annual shifts. Therefore, the highest and the lowest values of the net nitrogen fluxes (Figure 7) were capped at $-20 \text{ t N}_{\text{ges}}$ and $+20 \text{ t N}_{\text{ges}}$, respectively. After this step, the difference between total exports and total imports was only 3%.

For adjusting the NH_3 -emission map from manure application, the transported amount of N_{ges} was converted to the respective emission of $\text{NH}_3\text{-N}$ by a factor of 21%. This value was derived from results of the Agrammon model supplied by Bonjour & Kupper (2017); along with emission factors (EF, see Table 2) they calculated average fluxes of nitrogen fed to manure storage for different animal categories. The factor was calculated as: $(\text{EF of application}) / (\text{N to application})$ for dairy cows and fattening pigs and by weighting with the frequency of the farm class.

The influence of manure transport on ammonia emissions from manure application calculated per zip-code was spatially transferred to the agricultural areas where manure is primarily applied (i.e. orchards, horticulture, arable land, meadows and farm pastures) using a GIS-density function with a radius of 4 km. The

resulting map in Figure 8 confirms that ammonia emissions are generally translocated from areas with very high livestock densities to areas with lower densities. The total amounts of reductions and additions are 0.46 kt NH₃-N, corresponding to 3% of total emissions from manure application.

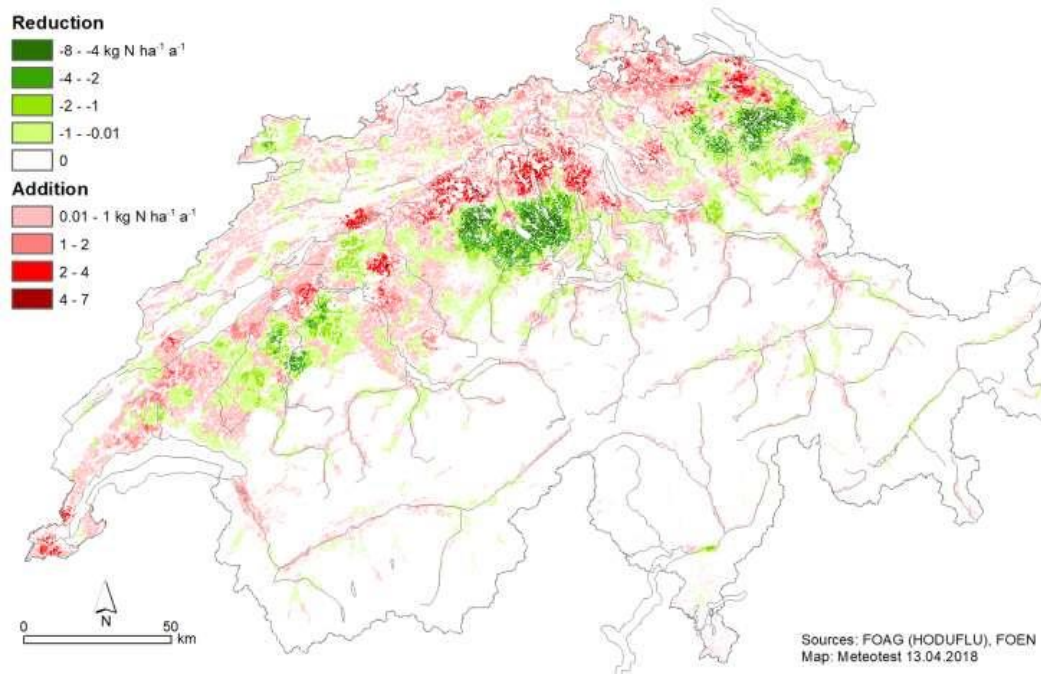


Figure 8: Reductions and additions of ammonia emissions from manure application caused by manure transports according to the HODUFLU database 2015 (FOAG 2017a).

d) Summering of animals on alpine pastures

For each farm, the livestock statistics (SFSO 2017) also provided the number of cattle, horses, sheep and goats spending the summer up on the alps (codes x3110 to x3465). The summering period is defined to last 100 days. In 2015, there were 22'226 farms reporting summering of animals. The emissions of those animals during summering were calculated with the stratified emission factors (Bonjour & Kupper 2017) for the stages housing, manure application and grazing by considering the relative length of the summering period (factor 100/365). As a best guess, it was assumed that the emissions by manure storage are not altered or relocated by summering.

The emissions by summering were subtracted from the yearly emissions of each farm reporting summering of animals; for further processing see chapter 3.4.1b. The total emission by summering in 2015 amounted to 1.944 kt NH₃-N. Figure 9 shows the origin of summered animals and corresponding emission subtractions. Most of the summered animals come from farms in the mountain valleys of the

Alps and Jura. But also in large parts of the Swiss Plateau, there are farms sending animals to the alps.

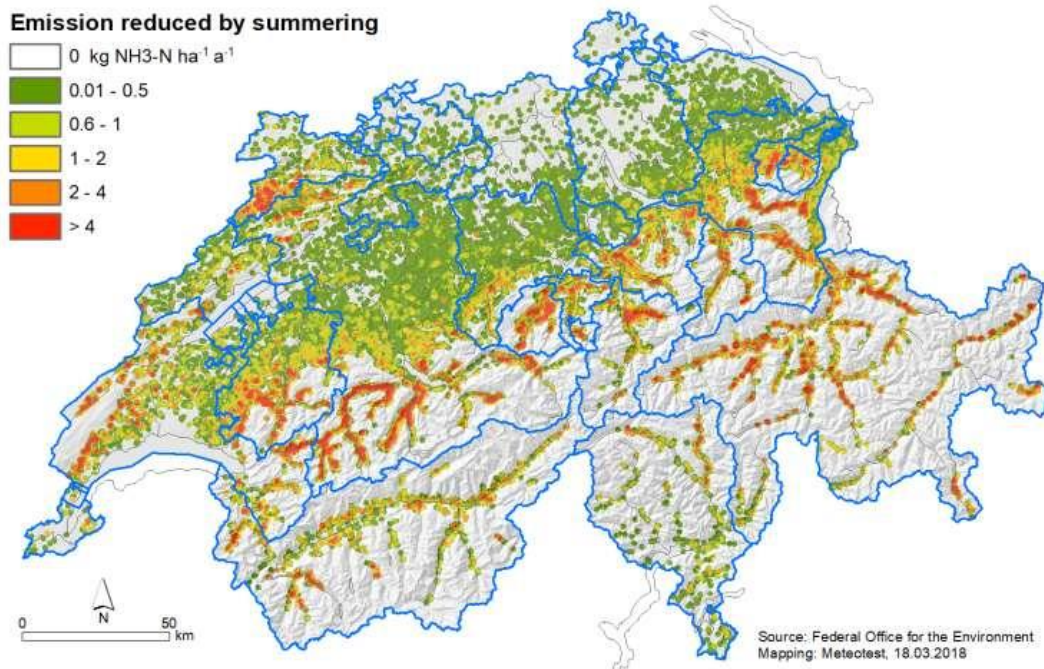


Figure 9: The emissions of summered animals are subtracted from the yearly emissions on each farm sending animals. The map shows these emission reductions; for better display a GIS-density function (radius 2 km) was applied.

As there was no explicit information where the summered animals exactly go to, further auxiliary data were used for mapping the summering emissions. We assumed that the summering emissions (1.944 kt NH₃-N) occur on the land-use category "alpine agricultural areas" (NOAS04 codes 45–49, SFSO 2013). The emission rates on those areas were weighted according to the expected intensity of summering activities.

For estimating the summering intensity, the database of the Swiss summering farms (*Sömmerungsbetriebe*, farms in operation only seasonally) was used as well (FOAG 2017b). The database contains the location of the summering farm (alp) and its regular carrying capacity expressed as NST (*Normalstoss*); NST is defined as one livestock unit (LSU, *Grossvieheinheiten GVE*) summered for 100 days. As can be seen in Figure 10, the database is quite heterogenous and data are missing for several cantons⁵; the map presents the result of a GIS-density function spreading the NST of each alp within a radius of 2 km (units NST/ha).

⁵ A further database (not considered at the time of modelling) with detailed information on summering farms has been published by SAB (*Schweizerische Arbeitsgemeinschaft für Berggebiete*): http://www.alporama.ch/gv2/get/get_ov_Kanton.asp

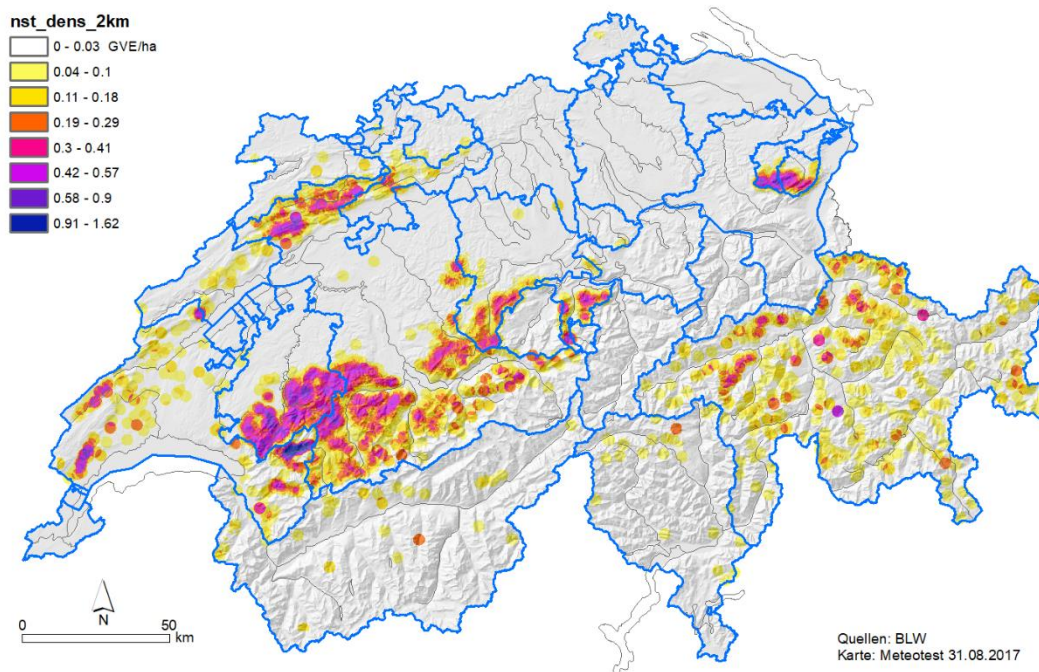


Figure 10: Carrying capacity of the summering farms (alps) provided by FOAG (2017b). The number of LSU per site were transformed to LSU/ha by a GIS-density function with radius 2 km. Blue lines: cantonal borders.

As the summering farm data were quite incomplete, further information on the possible weighting of alpine pastures was derived from the calculated emissions of the "sending" farms (see Figure 9): The summering-related emissions on the "sending" farms were dispersed by a density function within a radius of 8 km (units kg NH₃-N/ha). The result is shown in Figure 11 (weight sending farms); regions with a density of more than 0.4 kg NH₃-N/ha are highlighted.

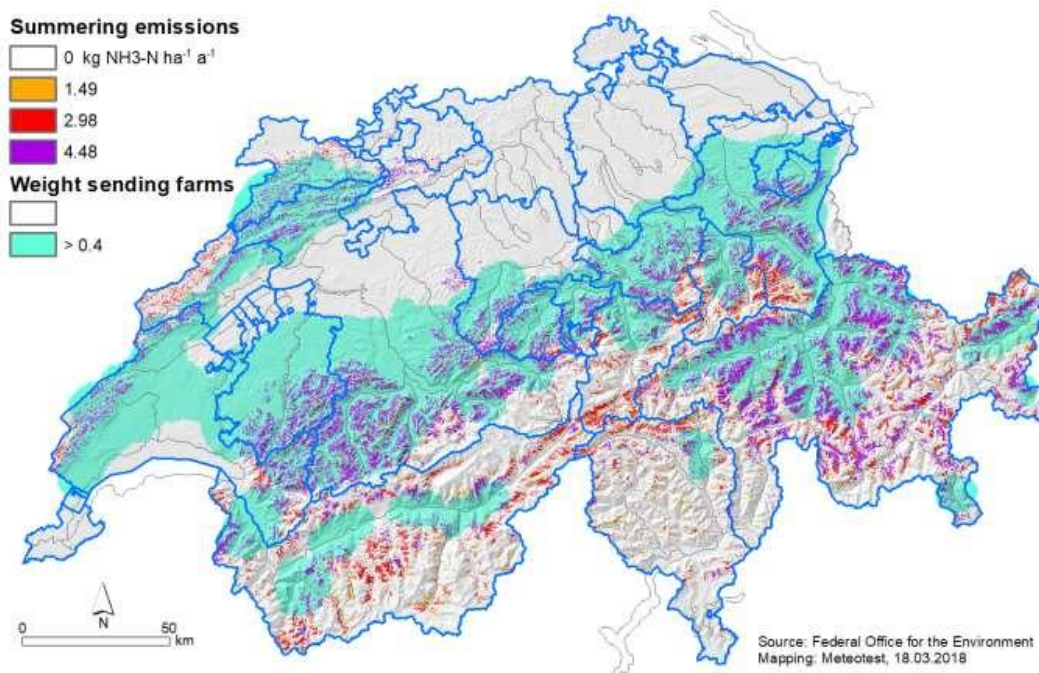


Figure 11: (1) Weight of farms sending the summering livestock calculated from the respective ammonia emissions by a density function with radius 8 km. (2) Ammonia emissions from alpine agricultural areas due to summering. (3) Blue lines: cantonal borders.

Finally, the alpine agricultural areas were weighted, with regard to ammonia emissions by summering, as follows (land-use codes in parenthesis):

- Weight = 0.33: sheep pastures (49).
- Weight = 0.66: remote areas that are covered by alpine meadows (45), favourable alpine pastures (46), brush alpine pastures (47) or rocky alpine pastures (48).
- Weight = 1.00: accessible areas that are covered alpine meadows (45), favourable alpine pastures (46), brush alpine pastures (47) or rocky alpine pastures (48).

The accessible areas were defined by a carrying capacity of the summering farms greater than 0.03 LSU/ha (Figure 10) or by a weight of the sending farm greater than 0.4 kg NH₃-N/ha (Figure 11). All other areas were considered as remote areas.

With the total summering emissions of 1.944 kt NH₃-N, the resulting emission rate for an area with a weight 1.00 is 4.48 kg NH₃-N/ha as shown on Figure 11.

e) Emissions from plant production

Emissions from the application of mineral fertilizer and organic recycling fertilizer (total 2.40 kt NH₃-N a⁻¹, see Table 1, adopted from FOEN 2017) were distributed over the land-use categories arable land (41), meadows (42), horticulture (40), vineyards (39), orchards (37, 38) and golf courses (33) using the land-use map by SFSO (2013).

Emissions on agricultural land arising from processes in the plant layer (total 2.34 kt NH₃-N a⁻¹, see Table 1, adopted from FOEN 2017) were allocated as follows:

- An emission factor of 2.0 kg NH₃-N ha⁻¹ was applied on agricultural land without alpine pastures (land-use codes 37–44). The resulting emission is 2.07 kt NH₃-N a⁻¹.
- An emission factor of 0.5 kg NH₃-N ha⁻¹ was applied on land-use categories alpine pastures (land-use codes 45–49). The resulting emission is 0.27 kt NH₃-N a⁻¹.

d) Non-agriculture emissions

Emissions from commerce and industry (0.46 kt NH₃-N a⁻¹, see Table 1, adopted from FOEN 2017) were distributed over the land-use categories 'industrial and commercial areas' (SFSO 2013, codes 1 and 2).

The ammonia emissions from road transportation (1.47 kt NH₃-N a⁻¹, see Table 1) were mapped by a bottom-up approach based on a traffic model for the year 2015 (INFRAS 2017) using updated methods and emission factors as described by BAFU (2010). The traffic model includes the main road-networks and zonal traffic. The emissions on the road-links (1.41 kt NH₃-N a⁻¹) were converted to a hectare raster. The zonal emissions (0.06 kt NH₃-N a⁻¹) were allocated to a ha-raster according to population density and settlement areas.

Emissions from households (0.85 kt NH₃-N a⁻¹, see Table 1, adopted from FOEN 2017) were distributed over the land-use categories for residential areas (codes 3–8), agricultural building areas (codes 11 and 12) and garden allotments (code 35).

Emissions from waste treatment (0.55 kt NH₃-N a⁻¹, see Table 1, adopted from FOEN 2017) were distributed over the land-use categories 'waste water treatment plants' and dumps (codes 25 and 27).

Natural emissions (0.60 kt NH₃-N a⁻¹, see Table 1, adopted from Kupper et al. 2013) originate from soil processes on natural grassland as well as from wild animals. They were distributed over the land-use categories wooded areas (codes 50–60) and unproductive vegetation (codes 64–67).

The total non-agricultural emissions (3.94 kt NH₃-N a⁻¹) are shown in Figure 12.

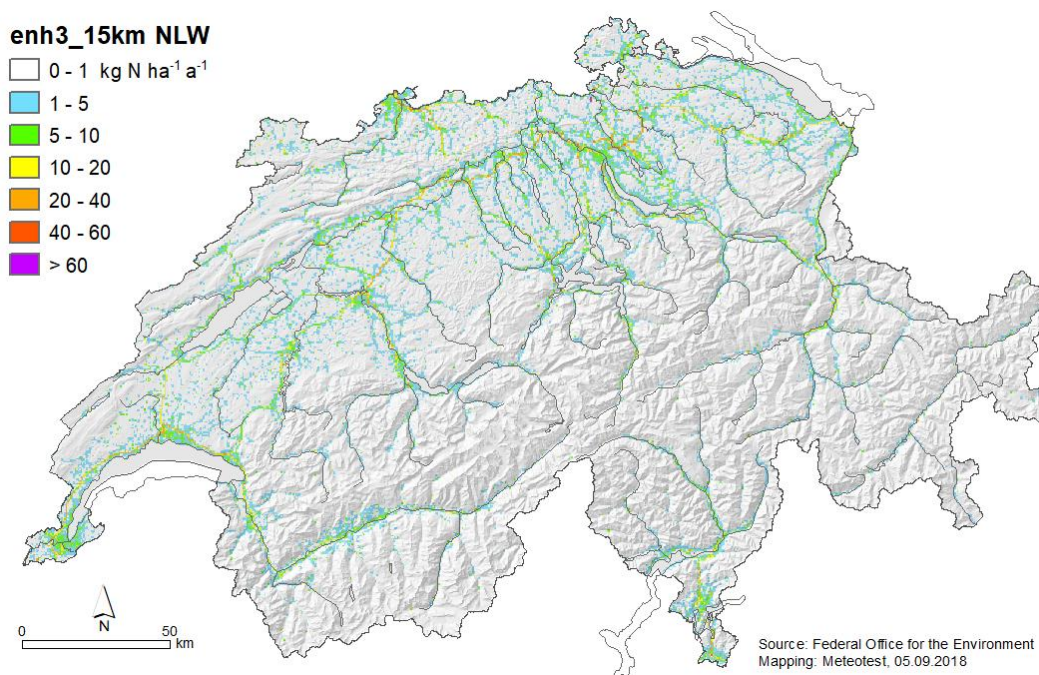


Figure 12: Non-agricultural ammonia emission 2015 modelled on a ha-raster.

3.4.2 Ammonia Concentration

A statistical dispersion model with a resolution of 100x100 m² was applied to calculate annual mean concentrations of ammonia in the air. It includes all emission sources at a maximum distance of 50 km. In doing so, abroad emissions were taken from a European dataset (JRC 2017). The model was set up as follows:

- The calculations are split in a local part and a regional part. The local part includes the ammonia sources within a maximum distance of 4 km to the receptor point; it is calculated on a ha-raster. The regional part represents the background concentration induced by the sources between 4 and 50 km distance to the receptor point; it is calculated on a 1x1km-raster.
- Normalised mean transfer functions were established; they provide the annual mean concentration (µg m⁻³) induced by a standard source of one kg NH₃ a⁻¹ depending on the distance and direction to the source; the functions are derived for different wind regions.
- The transfer functions are applied to all cells of the emission map to calculate an intermediate concentration map.

- The intermediate ammonia concentrations were compared with measured concentrations. The comparison showed a systematic effect of (relative) elevation which was included for calculating the final concentration map.

The method used to calculate the concentration C ($\mu\text{g m}^{-3}$) induced by the emissions from surrounding sources can be formulated as:

$$C = \sum_i \left(\frac{17}{14} \cdot E_i \cdot p(D_i, R_i) \right) \quad (\text{eq. 3.1})$$

where:

i	=	denotes all sources (raster-cells) within a radius of 50 km
E_i	=	NH_3 -emission from raster-cell i ($\text{kg NH}_3\text{-N a}^{-1}$), see Chapter 3.4.1
$17/14$	=	conversion from $[\text{kg NH}_3\text{-N}]$ to $[\text{kg NH}_3]$.
D_i	=	Distance to source i (m).
R_i	=	Direction to source i (azimuth).
$p(D, R)$	=	average transfer function; concentration as a function of D and R .

If the same frequency is assumed for all wind directions the transfer function depends on distance alone ($p(D)$, see Figure 14, left). This type of function was calculated by Asman & Jaarsveld (1990) using an atmospheric transport model. The model was applied and tested in several countries (The Netherlands, United Kingdom, Belgium, Denmark and Sweden) and in Europe (Asman & Jaarsveld 1992). In Switzerland, the integrated distance-function shown in Figure 13 and Equation 3.1 was used the first time by Rihm & Kurz (2001) to calculate NH_3 -concentration maps; the comparison with measured NH_3 -concentrations was promisingly good. Thus, the method was further developed and used for mapping NH_3 in Switzerland by EKL (2014) and Rihm & Achermann (2016).

The function $p(D)$ integrates effects of several atmospheric processes such as dilution by turbulence, deposition on the ground and chemical transformation of ammonia to ammonium. It is related to a point source at a height of 3 m above ground and the resulting concentrations are given for a reference height of 1 m above ground. In the present study, it was assumed that the sources and the receptor points are situated in the centre of the $100 \times 100 \text{ m}^2$ cells. For calculating the concentration in a raster-cell induced by the emission of the same cell (where $D = 0 \text{ m}$), a distance of 50 m was used in $p(D)$.

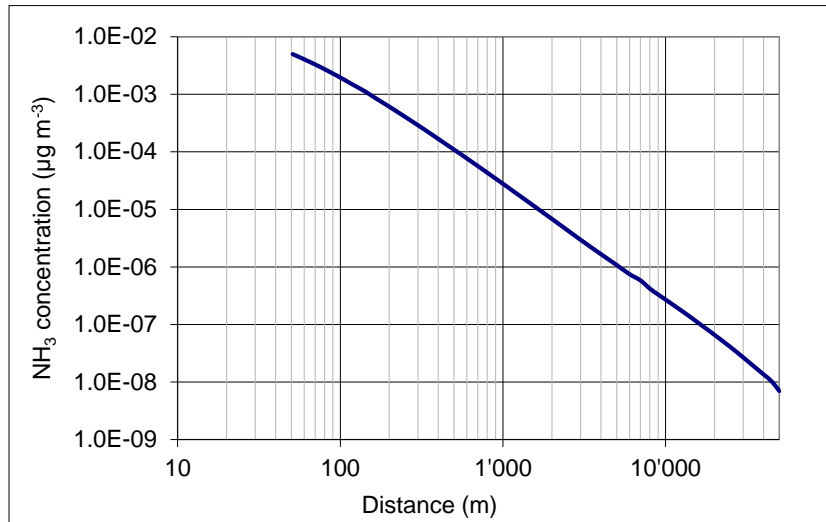


Figure 13: NH_3 concentration as a function of the distance to a source emitting $1 \text{ kg NH}_3 \text{ a}^{-1}$ for distances between 50 m and 50 km (by Asman & Jaarsveld 1990).

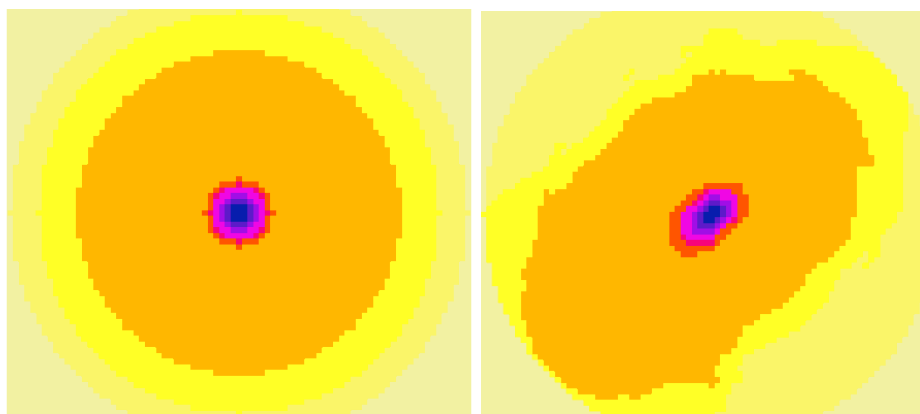


Figure 14: Schematic distance-functions. Left: rotation-symmetric use of $p(D)$ in the Alps. Right: modified $p(D, R)$ function according to prevailing wind directions in the Jura/Plateau region.

Furthermore, twelve different climatic regions were defined for the calculation of distances below 4 km (see Figure 15):

- In Northern Switzerland (covering the Jura Mountains and the Swiss Plateau) the $p(D)$ function was modified according to prevailing wind directions in this area (Figure 14, right); i.e. the concentration is calculated as a function of distance and direction between source and receptor. The modification was based on the region-specific dispersion profiles developed for NO_2 (FOEN 2011).
- At higher altitudes in the Alps and Southern Switzerland, the function $p(D)$ was applied rotation-symmetrically (Figure 14, left).

- In the Alpine valleys, the distance-functions was adjusted to the prevailing canalised wind directions as shown in Figure 15

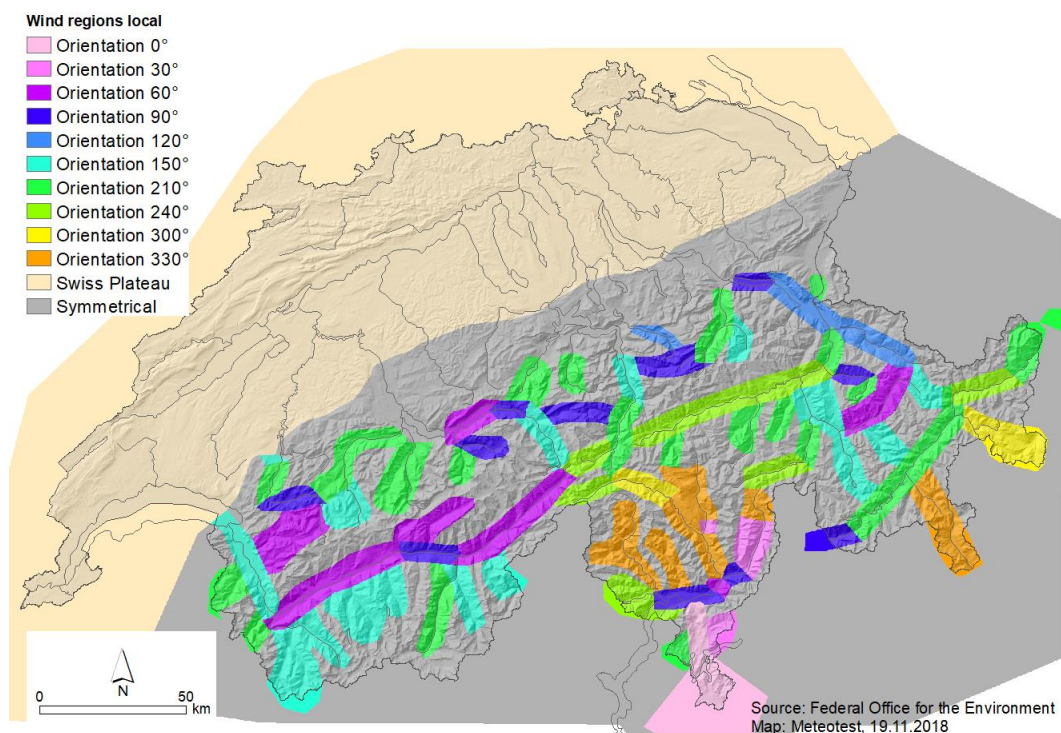


Figure 15: The twelve wind regions used for the local dispersion modelling (0–4 km distance from sources) with their prevailing wind direction.

For the regional modelling, four different climatic regions were defined as shown in Figure 16: Plateau/Jura, Basle, Alps and Southern Switzerland. The regional transfer functions were based on the Asman-Jaarsveld distance function (Figure 13) and modified using transfer functions that were developed for PM10 (FOEN 2013).

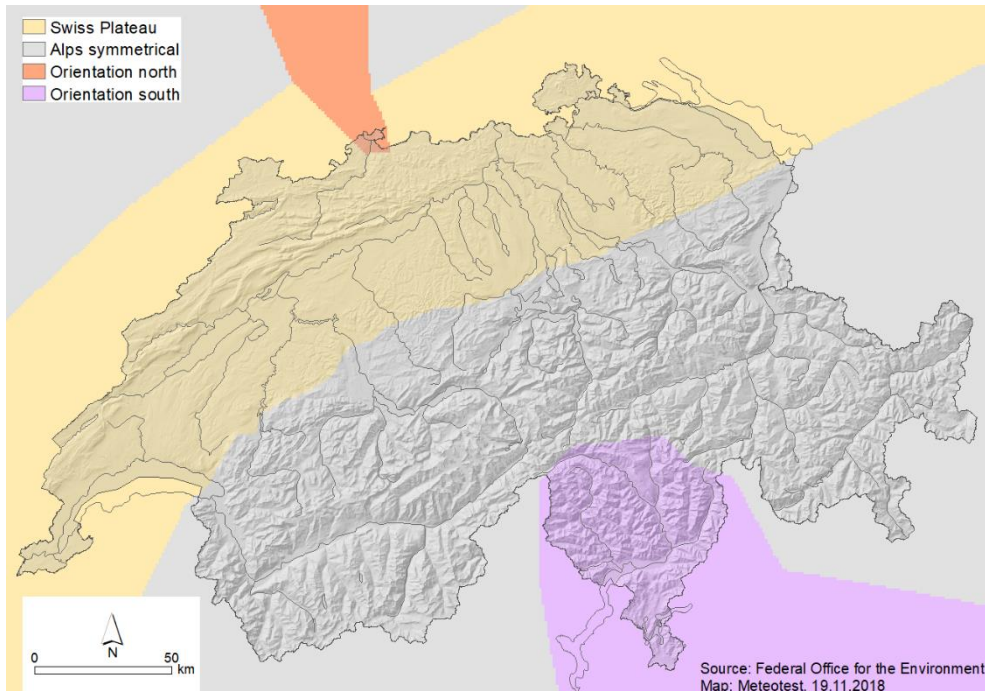


Figure 16: The four wind regions used for the regional dispersion modelling (4–50 km distance from sources).

There are 170 sites in Switzerland where ammonia concentrations were measured in the period 2013-2017 (Seitler 2018, Seitler et al. 2018). For the comparison with modelled data, the average concentration 2013-2017 at each measurement location was used. However, 22 sites were excluded in the comparison because their distance to the nearest farm was below 150 m: In this situation, a comparison is difficult as the location of the farms in the model is rasterized to 100x100 m².

In the comparison of modelled and measured ammonia concentrations, the residuals showed a systematic influence by topography. For further examination of the effect, the relative elevation (Hrel2) was used. Hrel2 was calculated as: elevation minus the minimum elevation within a radius of 2 km. In flat terrain, Hrel2 is 0 while in very steep topographic situation it can reach values over 1'000 m (Figure 17).

Figure 18 shows the relationship between the residuals (expressed as ratio modelled to measured) and Hrel2: In flat terrain, the model underestimates the concentrations and in steep terrain, the model overestimates the ammonia levels. This relation can be reasonably explained by effects that were not included in the model: (1) near-ground inversion layers and cold air pools that occur mainly in flat terrain and lead to an increase of ammonia concentrations, and (2) the canalising effect of slopes in steep terrain inhibiting uphill dispersion.

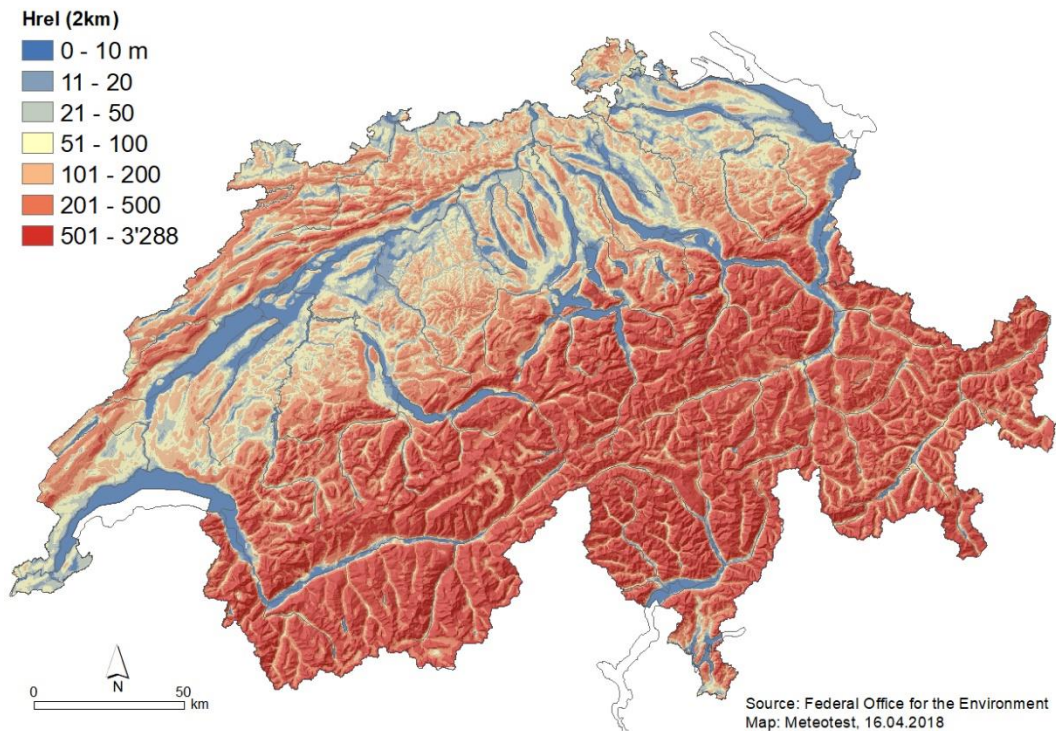


Figure 17: Relative elevation Hrel2 (elevation minus minimum elevation within a radius of 2 km).

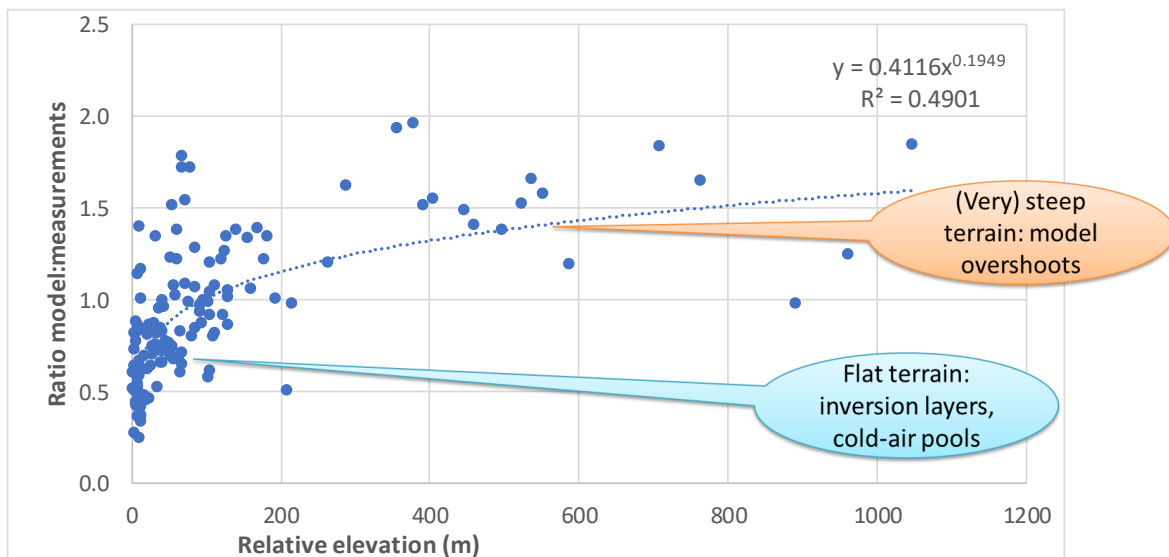


Figure 18: Relationship between the residuals (ratio modelled to measured ammonia concentrations) and the relative elevation (Hrel2).

A topographic correction factor was calculated for each raster cell using Hrel2 and the regression function shown in Figure 18 within the limits 0.55–1.5 or 4–

800 m, respectively. The resulting map of ammonia concentrations in 2015 after this topographic correction is shown in Figure 19 and the comparison with measurements in Figure 20. With the topographic correction R^2 of the linear regression improves from 0.55 (not shown) to 0.73.

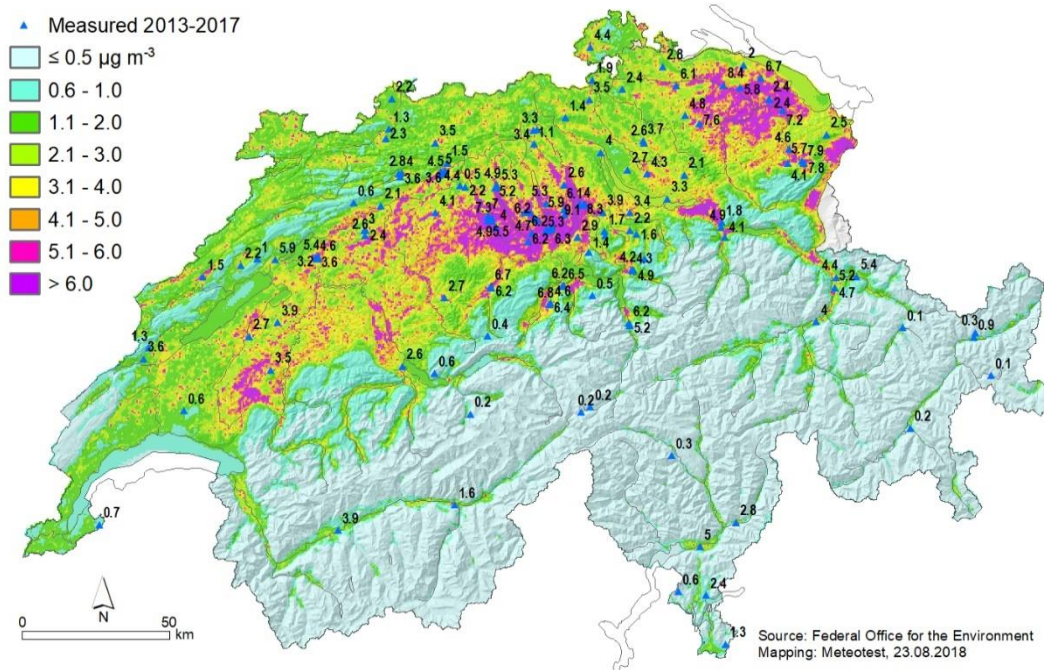


Figure 19: Map of NH₃ concentration in 2015 (100 x 100 m² raster) and monitoring sites.

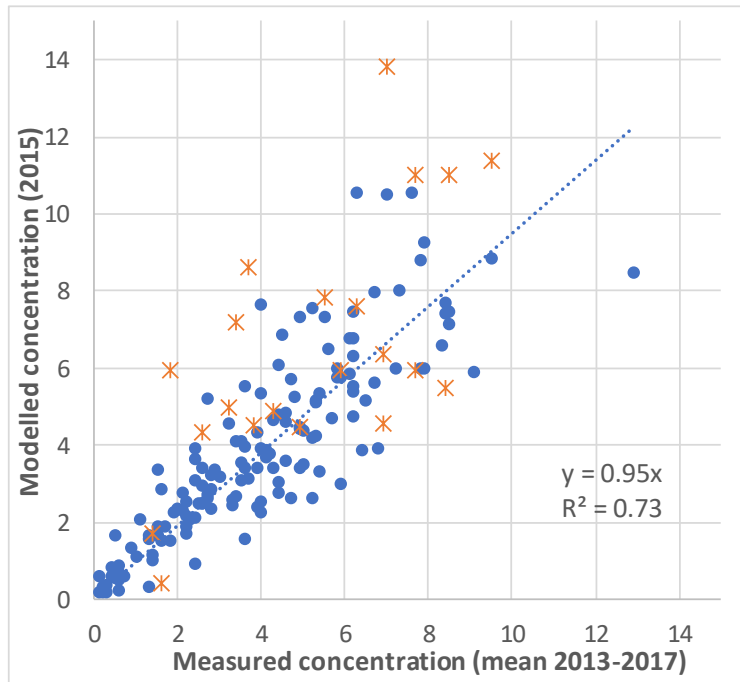


Figure 20: Comparison of measured and modelled ammonia concentrations ($\mu\text{g m}^{-3}$), $n=148$ (blue markers). The monitoring sites with distances <150 m to farms or obviously incorrect farm coordinates were not included into the regression (red markers).

3.5 Updates of the Maps 1990, 2000, 2005 and 2010

The deposition maps for the previous years calculated by Rihm & Achermann (2016) were updated as follows:

- The year 2005 is now reported instead of 2007. This was obtained by calculating wet deposition as average 2003–2007 and gaseous deposition of NO_2 as average 2004–2006. However, the original ammonia map based on livestock statistics 2007 was not revised.
- Updated NO_2 -concentration maps were used (BAFU 2017), and for calculating gaseous NO_2 -deposition, the 3-year averages 1999–2001, 2004–2006 and 2009–2011 were used for the years 2000, 2005 and 2010, respectively.
- The NH_3 -concentration maps 1990–2010 were adjusted with a topographic correction factor as shown in chapter 3.4.2 within the limits 0.63–1.5.
- Wet deposition 1990–2010 in Northern Switzerland was recalculated using a west-east gradient of concentrations in precipitation as shown in chapter 3.2.
- Wet deposition 1990–2010 in Southern Switzerland was recalculated using updated regression results supplied by Steingruber (2018).

- Due to lacking data, manure transport and summering of livestock could not be considered for 1990–2010.

4 Results

For the years 1990, 2000, 2005 and 2010 updated maps of ammonia concentration, total N deposition and (maximum) exceedances were produced. They are shown together with the new maps for 2015 in Annex B.

4.1 Critical Loads of Nitrogen

Figure 21 shows the resulting map of the empirical critical loads ($CL_{emp}(N)$) with the minimum critical loads occurring in each 1x1 km² cell. The following ecosystems were included (see also Rihm & Achermann 2016): raised bogs (HM), fens (FM), dry grassland (TWW), selected vegetation types by Hegg et al. (1993), hay meadows (biodiversity monitoring) and alpine lakes.

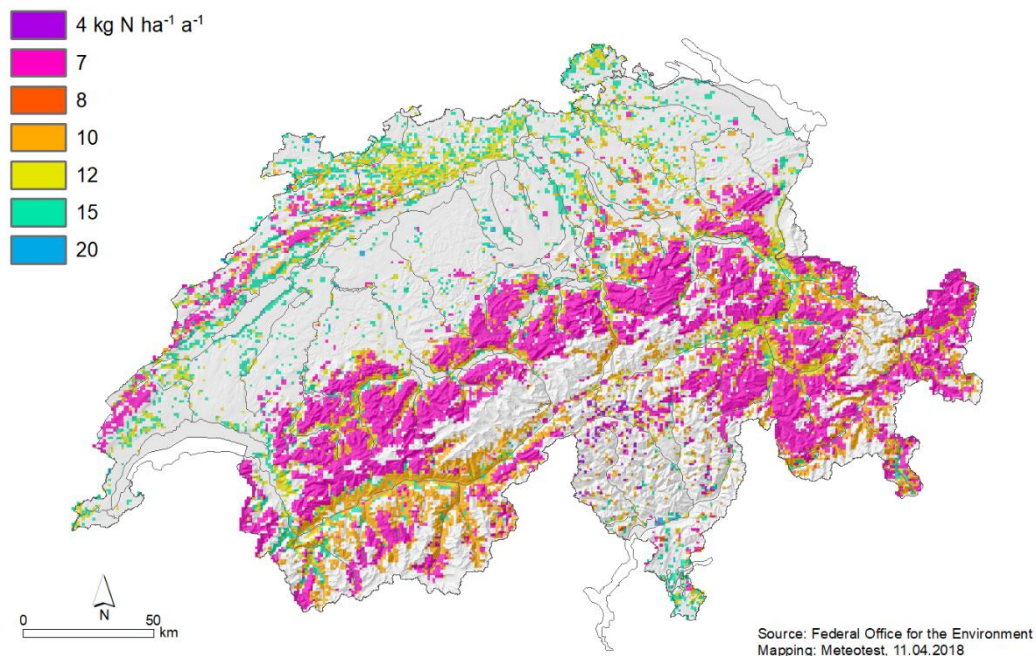


Figure 21: Revised map of the empirical critical loads ($CL_{emp}(N)$) in Switzerland.

The critical loads of nutrient nitrogen for forests ($CL_{nut}(N)$) calculated with the Simple Mass Balance were not revised in this study. However, the values provided by Rihm & Achermann (2016) were used to produce the combined map shown in Figure 22.

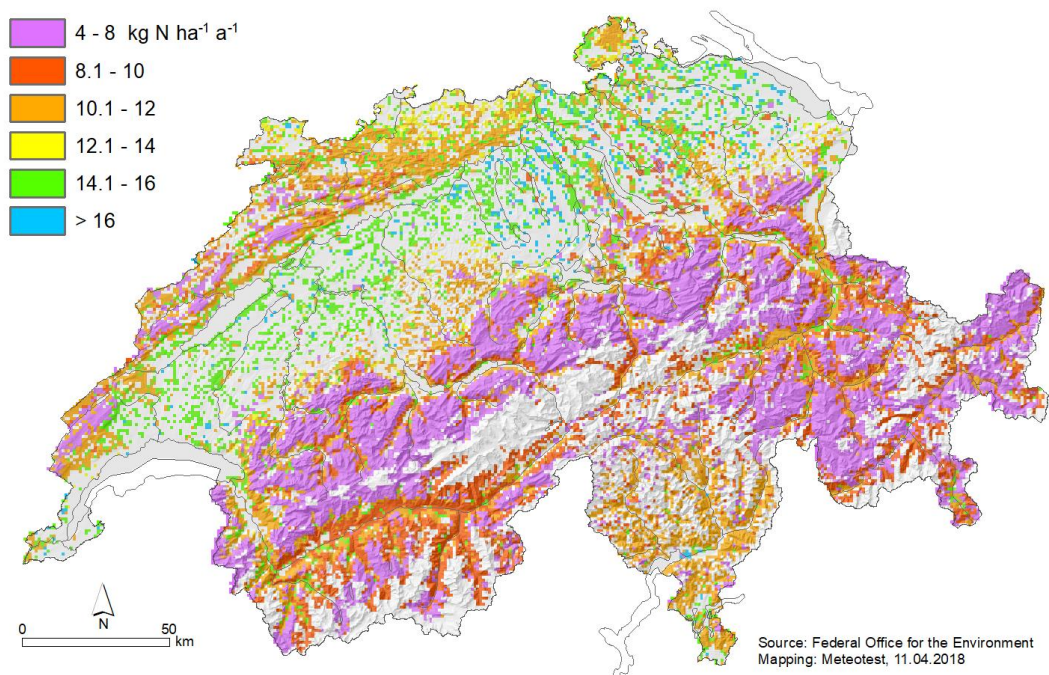


Figure 22: Revised map of combined critical loads calculated as minimum of $CL_{emp}(N)$ and $CL_{nut}(N)$ per km^2 .

4.2 Deposition of Nitrogen

The modelled nitrogen depositions in 2015 are displayed in Figure 23. As shown in Table 4, the resulting total nitrogen deposition in Switzerland for the year 2015 amounts to 61.7 kt N a^{-1} ($15.0 \text{ kg ha}^{-1} \text{ a}^{-1}$) to which gaseous NH_3 contributes 37%, wet NH_4^+ 26%, wet NO_3^- 17%, gaseous NO_2 10%, dry NH_4^+ 5%, gaseous HNO_3 3% and dry NO_3^- 2%. The share of reduced nitrogen compounds ($\text{NH}_y\text{-N}$) is 68%. A recent study by Thimonier et al. (2018) showed that the total N deposition modelled for forest stands generally matches well the measured values.

Table 4: Total deposition of N compounds in Switzerland 2015.

Receptors		Forest 11'401 km ²		Non-forest 29'683 km ²		Total 41'264 km ²	
Compounds							
Wet:	NH ₄ ⁺	5.2	4.5	10.9	3.7	16.1	3.9
Dry:	NH ₄ ⁺ aerosol	1.4	1.2	1.5	0.5	2.9	0.7
	NH ₃ gas	9.0	7.9	13.7	4.6	22.7	5.5
Total NH_y-N:		15.6	13.7	26.1	8.7	41.7	10.1
Wet:	NO ₃ ⁻	3.4	3.0	7.0	2.4	10.4	2.5
Dry:	NO ₃ ⁻ aerosol	0.6	0.5	0.6	0.2	1.2	0.3
	NO ₂ gas	3.0	2.7	3.2	1.1	6.2	1.5
	HNO ₃ gas	0.6	0.5	1.5	0.5	2.1	0.5
Total NO_y-N:		7.6	6.7	12.4	4.1	20.0	4.8
Total N		23.2	20.4	38.5	12.9	61.7	15.0

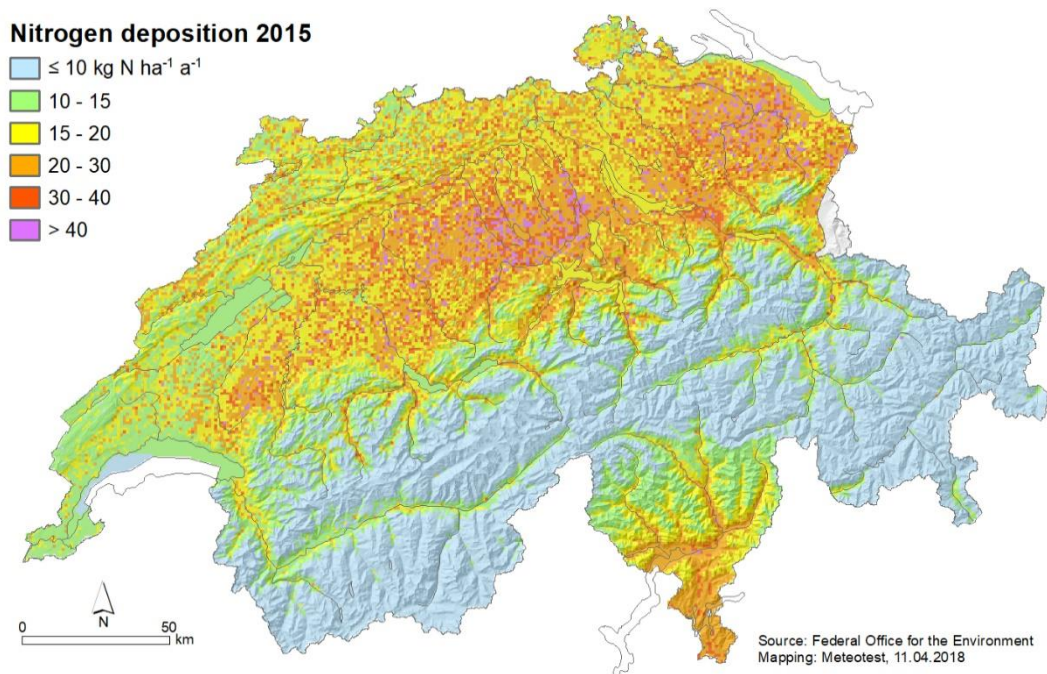


Figure 23: Total deposition of nitrogen calculated on a 1 x 1 km² raster.

Table 5 and Figure 24 give an overview of the deposition development 1990–2015: In this period total N deposition in Switzerland decreased by 28%. Figure 24 also shows the respective model results from EMEP (based on a 50x50km grid): While the results for 2010–2015 are quite comparable (EMEP 7% lower) the development of reduced nitrogen between 1990 and 2010 calculated by EMEP is difficult to interpret.

Table 5: Total deposition of N compounds in Switzerland; years 1990–2015. Units: kt N a⁻¹.

Compounds		1990	2000	2005	2010	2015
Wet:	NH ₄ ⁺	24.4	21.3	19.5	17.4	16.1
Dry:	NH ₄ ⁺ aerosol	2.9	2.9	2.9	2.9	2.9
	NH ₃ gas	26.8	24.0	24.0	23.6	22.7
<i>Total NH_y-N:</i>		<i>54.2</i>	<i>48.3</i>	<i>46.5</i>	<i>43.9</i>	<i>41.7</i>
Wet:	NO ₃ ⁻	18.4	14.6	12.5	12.0	10.4
Dry:	NO ₃ ⁻ aerosol	1.2	1.2	1.2	1.2	1.2
	NO ₂ gas	9.2	7.4	7.3	7.0	6.2
	HNO ₃ gas	2.4	2.1	2.1	2.1	2.1
<i>Total NO_y-N:</i>		<i>32.0</i>	<i>25.4</i>	<i>23.1</i>	<i>22.3</i>	<i>20.0</i>
<i>Total N</i>		<i>86.3</i>	<i>73.3</i>	<i>69.6</i>	<i>66.2</i>	<i>61.7</i>
<i>Total N, percent</i>		<i>100%</i>	<i>86%</i>	<i>82%</i>	<i>78%</i>	<i>72%</i>

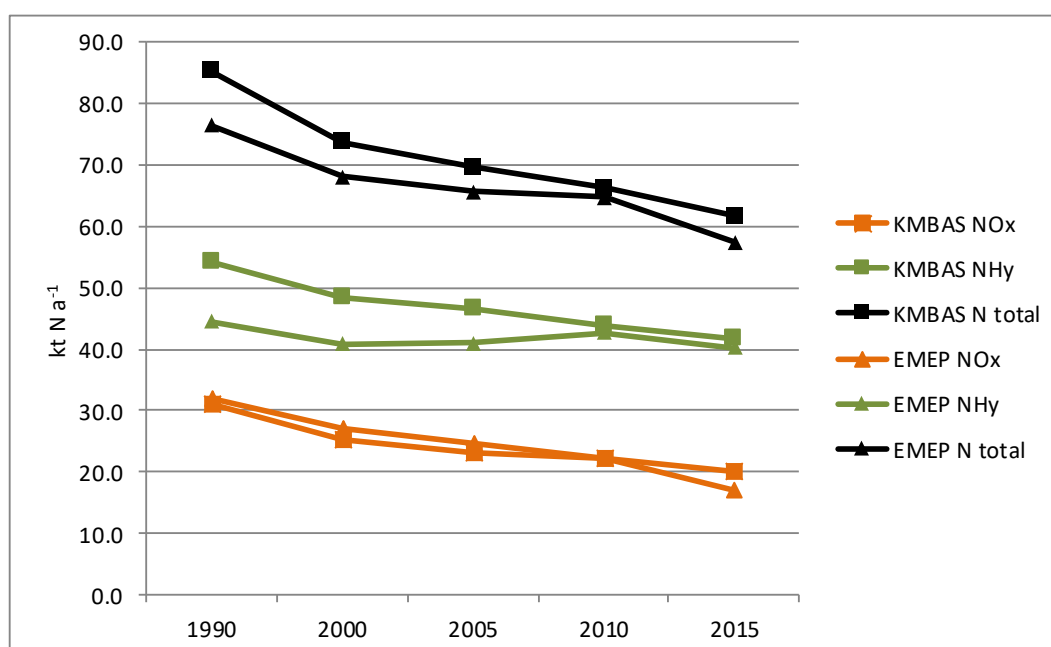


Figure 24: Total nitrogen deposition 1990–2015 in Switzerland calculated by EMEP (EMEP 2018, Gauss et al. 2016) and by the national model (KMBAS).

4.3 Exceedances of Critical Loads of Nitrogen

The map in Figure 25 displays the exceedances of empirical critical loads in 2015. It shows the exceedance of the most sensitive (semi-)natural ecosystem type occurring in each 1 x 1 km² raster cell. Figure 26 shows the exceedances of critical loads for productive forests calculated with the SMB method in 2015. The

map in Figure 27 combines the exceedance of the critical loads for (semi-)natural ecosystems and forests showing the maximum exceedance per 1 x 1 km² raster cell.

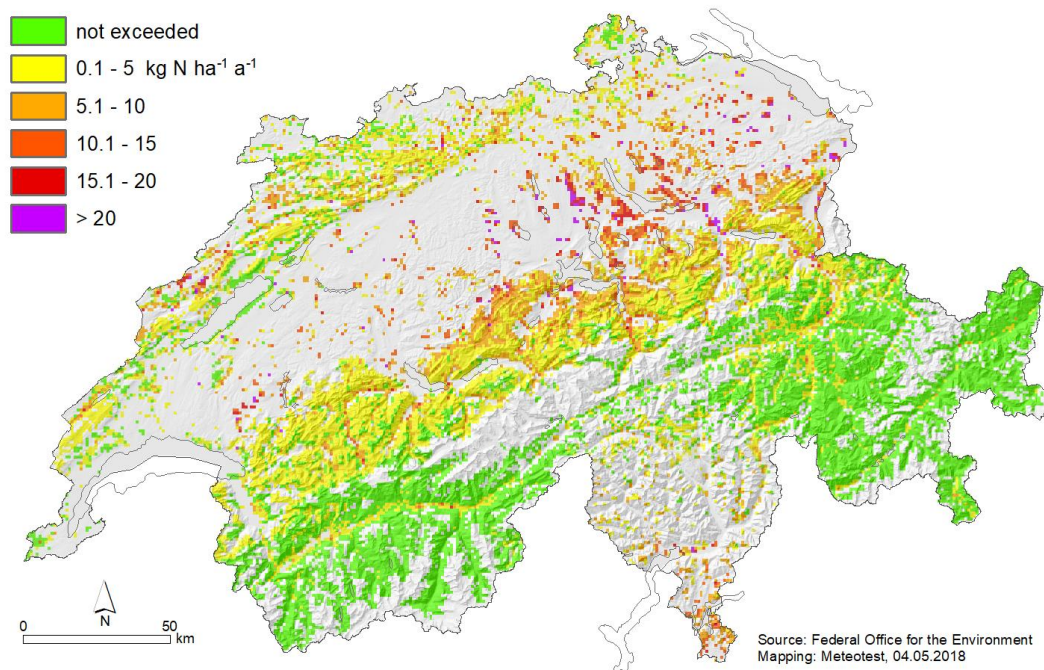


Figure 25: Exceedance of critical loads for (semi-)natural ecosystems ($CL_{emp}(N)$) by nitrogen depositions in 2015.

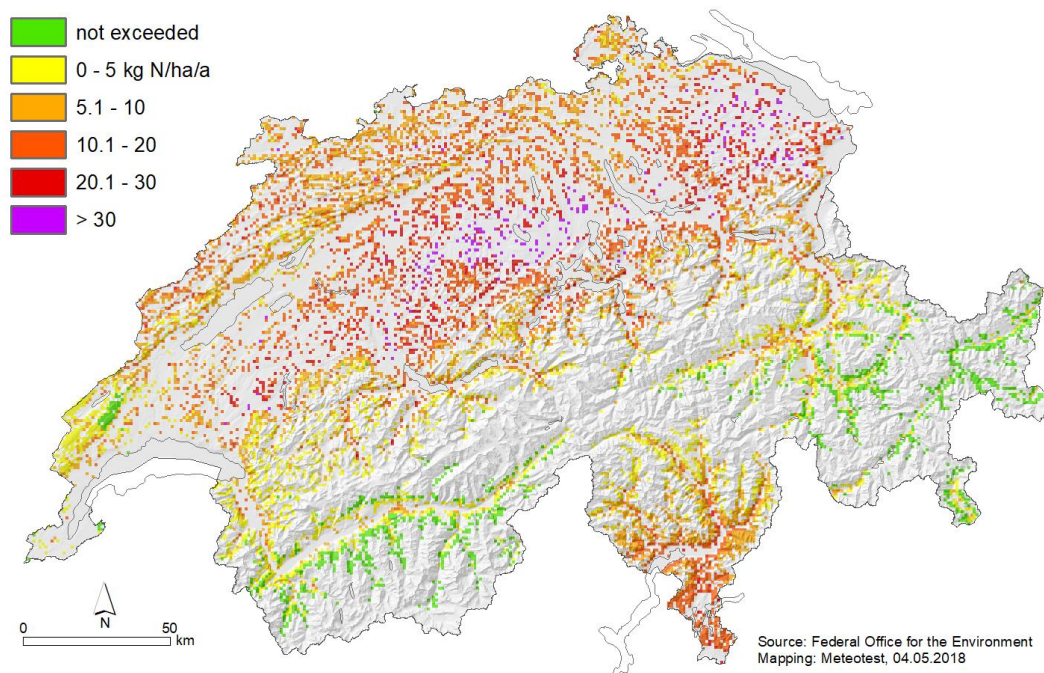


Figure 26: Exceedance of critical loads for productive forests ($CL_{nut}(N)$) by nitrogen depositions in 2015. Forest grid: WSL 1990/92.

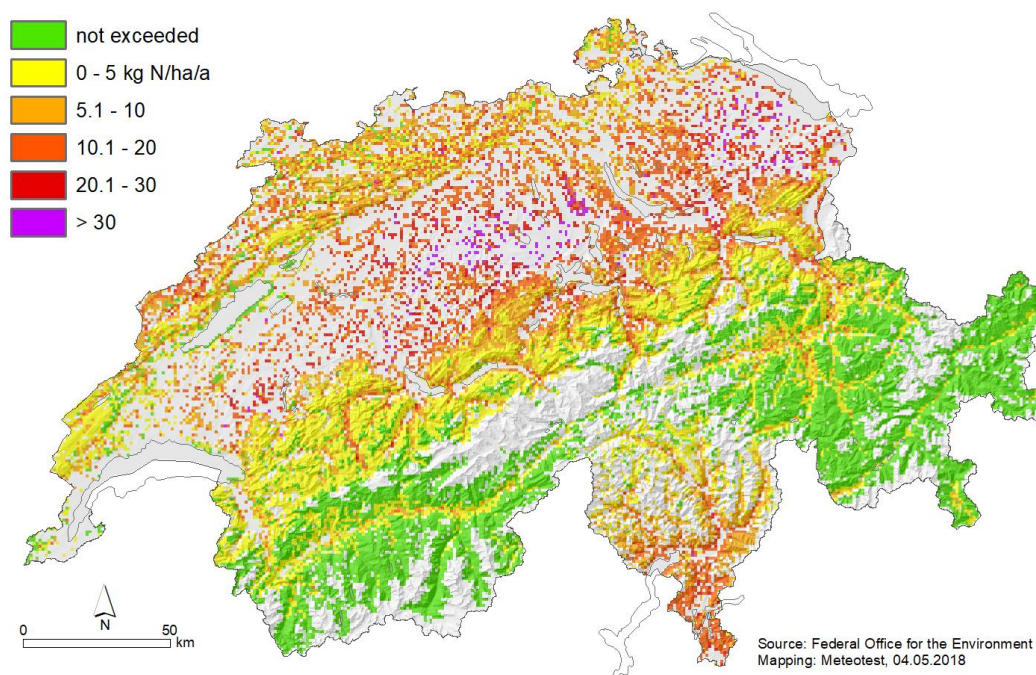


Figure 27: Combined map showing the maximum exceedance of critical loads for forests ($CL_{nut}(N)$) and (semi-)natural ecosystems ($CL_{emp}(N)$) by nitrogen depositions in 2015 per 1 x 1 km² raster cell.

Table 6 shows the exceedances calculated on the 1x1 km² raster for the whole period 1990–2015.

Table 6: Exceedance of critical loads (percent of the ecosystem area) on the 1x1 km² raster.

Critical load	Area ^a (km ²)	1990	2000	2005	2010	2015
Empirical CLN, (semi-) natural ecosystems	18'287	79	70	63	61	55
SMB CLN, productive forest	10'457	97	94	92	92	89
Maximal (combined) exceedance ^b per km ²	23'673	85	79	74	74	69

^a area of raster cells containing (semi-) natural ecosystems and productive forests, this does not mean that the surface is entirely covered by these ecosystems.

^b considering the most sensitive ecosystem type per raster cell.

Table 7 presents the exceeded area for the most important sensitive nature conservation areas in Switzerland (raised bogs, fens, dry grassland and forest). For this analysis, the critical loads (according to Chapter 2), deposition and the resulting exceedance were calculated on a 100x100 m² raster (cf. EKL 2014). For for-

ests, the exceedance was calculated on the 1x1 km² sampling points of the national forest inventory as shown in Figure 26 (WSL 1990/92). The values 1990–2010 (grey colour) originate from Rihm & Achermann (2016), i.e. they were not recalculated.

Cumulative frequency distributions of the exceedance for the year 2015 are shown in Figure 28.

Table 7: Exceedance of critical loads of nutrient nitrogen for different protected ecosystems in Switzerland. Units: percent of total ecosystem area.

Ecosystem	Area (km ²)	1990 ¹	2000 ¹	2010 ¹	2015
Raised bogs (HM)	57	100	100	98	94
Fens (FM)	215	91	82	76	77
Dry grassland (TWW)	253	81	62	49	36
Productive forest	10'288	99	96	95	87

¹ Cited from Rihm & Achermann (2016), i.e. not recalculated with the updated ecosystem inventories and deposition maps.

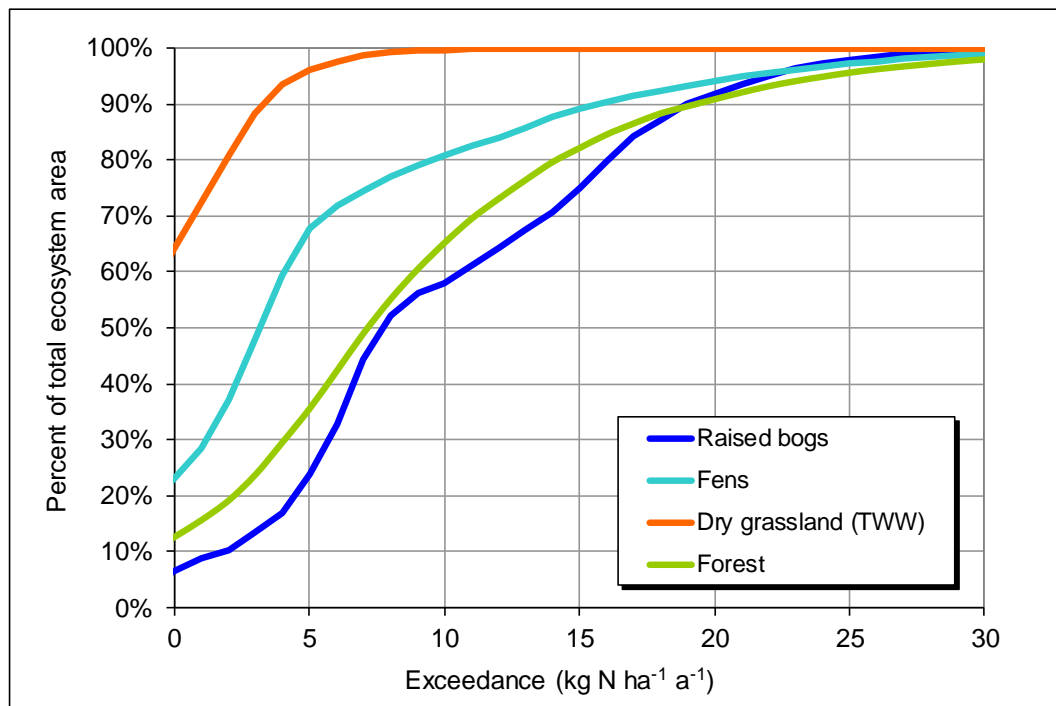


Figure 28: Cumulative frequency distribution of the exceedances of critical loads of nutrient nitrogen for different protected ecosystems. Units: percent of total ecosystem area. Nitrogen deposition: year 2015.

A References

Asman W.A.H. and van Jaarsveld H.A., 1990: A Variable-resolution Statistical Transport Model Applied for Ammonia and Ammonium, National Institute of Public Health and Environmental Protection (RIVM), Bilthoven, The Netherlands.

Asman W.A.H. and van Jaarsveld H.A., 1992: A variable-resolution transport model applied for NH_x in Europe. Atmospheric Environment Vol. 26A, No. 3, 445-464.

BAFU 2010: Luftschadstoff-Emissionen des Strassenverkehrs 1990–2035, Aktualisierung 2010, Umweltwissen Nr.1021, INFRAS im Auftrag des Bundesamts für Umwelt, Bern.
<https://www.bafu.admin.ch/bafu/de/home/themen/luft/publikationen-studien/publikationen/luftschadstoff-emissionen-des-strassenverkehrs-1990-2035.html>

BAFU 2017: Karten von Jahreswerten der Luftbelastung in der Schweiz - Datengrundlagen, Berechnungsverfahren und Resultate der Karten bis zum Jahr 2016. Report by Meteotest, 01.09.2017, on behalf of the Federal Office for the Environment (Bundesamt für Umwelt BAFU), Bern. <https://www.bafu.admin.ch/bafu/en/home/topics/air/state/data/historical-data/maps-of-annual-values.html> [22.08.2018]

Barbieri A., and Pozzi S., 2001: Acidifying deposition, Southern Switzerland. Environmental Documentation - Air, Vol. 134, Swiss Agency for the Environment, Forests and Landscape (SAEFL), Bern, 113 p.

Bonjour C., Kupper T. 2017: Stratified emission factors for 24 animal categories, emission stages and farm classes; results from the Agrammon-project. Pers. comm. Cyrill Bonjour and Thomas Kupper, HAFL Zollikofen, 20.11.2017.

EMEP 2018: National totals and gridded data. Downloaded from
http://www.emep.int/mscw/mscw_ydata.html#ASCIIdata

FOAG 2017a: Anonymized delivery receipts for the manure shipments in 2015; extract from the HODUFLU database. Federal Office for Agriculture (FOAG), Bern.
<https://www.blw.admin.ch/blw/de/home/politik/datenmanagement/agate/hoduflu.html>
<https://www.blw.admin.ch/blw/de/home/politik/datenmanagement/hoduflu.html>
<https://www.agrarbericht.ch/de/politik/datenmanagement/hoduflu-datenauswertung>
[5.4.2018]

FOAG 2017b: Location of alpine summering farms in 2015; extract from the AGIS-database. Federal Office for Agriculture (FOAG), Bern.
<https://www.blw.admin.ch/blw/de/home/instrumente/direktzahlungen/voraussetzungen-begriffe/soemmerungsbetriebe.html> [5.4.2018]

FOEN, 2011: NO₂ ambient concentrations in Switzerland. Modelling results for 2005, 2010, 2015. Federal Office for the Environment, Bern. Environmental studies no. 1123: 68 pp. <https://www.bafu.admin.ch/bafu/en/home/topics/air/publications-studies/publications/no2-ambient-concentrations-in-switzerland.html> [28.06.2017]

FOEN, 2013: PM10 and PM2.5 ambient concentrations in Switzerland. Modelling results for 2005, 2010 and 2020. Federal Office for the Environment, Bern. Environmental studies no. 1304: 83 pp. <https://www.bafu.admin.ch/bafu/en/home/topics/air/publications-studies/publications/pm10-and-pm2-5-ambient-concentrations-in-switzerland.html>

FOEN (ed.) 2017: Switzerland's Informative Inventory Report 2017 (IIR) – Submission under the UNECE Convention on Long-range Transboundary Air Pollution. www.ceip.at/ms/ceip_home1/ceip_home/status_reporting/2016_submissions

Gauss M., Nyíri Á, Benedictow A., and Klein H. 2016: Transboundary air pollution by main pollutants (S, N, O₃) and PM in 2014, Switzerland. MSC-W Data Note 1/2016 Individual Country Reports. EMEP; Norwegian Meteorological Institute. http://emep.int/mscw/mscw_publications.html [11.04.2018]

Hunziker C. 2018: Vegetation data for fens and dry grasslands from the Biotope Programme of the Federal Office for the Environment. Pers. comm. Christophe Hunziker, Yverdon-les-Bains, 07.03.2018.

INFRAS 2017: Swiss ammonia emissions 2015 from transportation, results of a link-based traffic model. Pers. comm. by B. Notter, 31.08.2017.

JRC 2017: EDGAR – Emissions Database for Global Atmospheric Research. Download of NH₃ data from http://edgar.jrc.ec.europa.eu/gallery.php?release=v431_v2&substance=NH3§or=TOTALS [17.01.2019]

Kupper T., Bonjour C., Achermann B., Rihm B., Zaucker F., Menzi H. 2013: Ammoniakemissionen in der Schweiz 1990–2010 und Prognose bis 2020. Hochschule für Agrar-, Forst- und Lebensmittelwissenschaften (HAFL). Bericht im Auftrag des BAFU.

Kupper T., Bonjour C., Menzi H., Bretscher D., Zaucker F. 2018: Ammoniakemissionen der schweizerischen Landwirtschaft 1990-2015. Bericht im Auftrag des BAFU. <https://agrammon.ch/dokumente-zum-download>

MeteoSwiss 2018: Supply of annual precipitation maps 2013-2017, 1x1 km² resolution. <http://www.meteoswiss.admin.ch/home/services-and-publications/produkte.subpage.html/en/data/products/2014/raeumliche-daten-niederschlag.html> [5.4.2018]

NABEL 2018: Supply of annual pollutant concentration and deposition in precipitation from the National Air Pollution Monitoring Network for (NABEL). Pers. comm. 07.03.2018, Federal Office for the Environment, Bern. <https://www.bafu.admin.ch/bafu/en/home/topics/air/state/data/national-air-pollution-monitoring-network--nabel-.html> [22.08.2018]

Rihm B., Achermann B. 2016: Critical Loads of Nitrogen and their Exceedances. Swiss contribution to the effects-oriented work under the Convention on Long-range Transboundary Air Pollution (UNECE). Federal Office for the Environment, Bern. Environmental Studies no. 1642: 78p. <https://www.bafu.admin.ch/bafu/en/home/topics/air/publications-studies/publications/Critical-Loads-of-Nitrogen-and-their-Exceedances.html> [5.4.2018]

Seitler E., Thöni L., Meier M., 2016: Atmosphärische Stickstoff-Deposition in der Schweiz, 2000 bis 2014. FUB – Forschungsstelle für Umweltbeobachtung, Rapperswil. <https://www.bafu.admin.ch/bafu/de/home/themen/luft/fachinformationen/luftqualitaet-in-der-schweiz/stickstoffhaltige-luftschadstoffe-beeintraechtigen-auch-die-biod.html> (Dokumente) [22.08.2018]

Seitler E. 2018: Ammonia concentrations measured with passive samplers, 2013-2017. Pers. comm. Eva Seitler, Forschungsstelle für Umweltbeobachtung (FUB), Rapperswil, 8.3.2018.

Seitler E., Meier M., Thöni L., 2018: Ammoniak-Immissionsmessungen in der Schweiz 2000 bis 2017, Messbericht. FUB – Forschungsstelle für Umweltbeobachtung, Rapperswil. <https://www.bafu.admin.ch/bafu/de/home/themen/luft/fachinformationen/luftqualitaet-in-der-schweiz/stickstoffhaltige-luftschadstoffe-beeintraechtigen-auch-die-biod.html> (Dokumente) [20.09.2018]

SFSO 2013: Swiss Land-Use Statistics (Arealstatistik), hectare raster with 72 basic categories. Swiss Federal Statistical Office (SFSO), Neuchâtel. <https://www.bfs.admin.ch/bfs/de/home/dienstleistungen/geostat/geodaten-bundesstatistik/boden-nutzung-bedeckung-eignung/arealstatistik-schweiz.html> [24.08.2018]

SFSO 2017: Livestock statistics of individual farms for 2015; database extract (Landwirtschaftliche Betriebszählungen). Swiss Federal Statistical Office (SFSO), Neuchâtel. <https://www.bfs.admin.ch/bfs/de/home/statistiken/kataloge-datenbanken/medienmitteilungen.assetdetail.40797.html> [22.08.2018]

Steingruber S. 2018a, Acidifying Deposition in Southern Switzerland - Monitoring, maps and trends 1983-2017, Cantone Ticino, Ufficio dell'aria, del clima e delle energie rinnovabili. https://www4.ti.ch/fileadmin/DT/temi/aria/monitoraggio/Acidifying_Deposition_Southern_Switzerland_1983-2017.pdf [17.01.2019]

Steingruber S. 2018b: Equations for calculating nitrogen concentration in precipitation in the Canton Ticino, 1988-2017. Pers. comm. April 20 2018.

swisstopo, 2006: Gemeindegrenzen, Nachführungsinfo 2006 zum Datensatz GG25. swissBOUNDARIES3D, geographic dataset. <https://shop.swisstopo.admin.ch/de/products/landscape/boundaries3D> [16.11.2018]

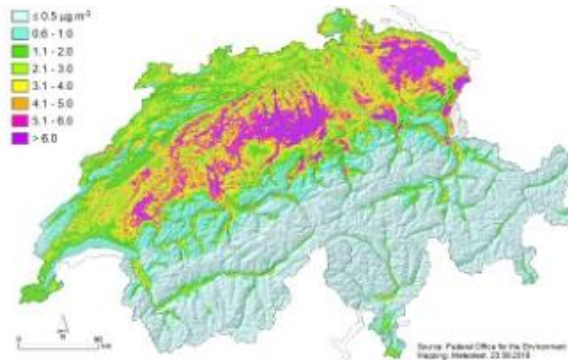
Thimonier A., Kosonen Z., Braun S., Rihm B., Schleppi P., Schmitt M., Seitler E., Waldner P., Thöni L. 2018: Total deposition of nitrogen in Swiss forests: Comparison of assessment methods and evaluation of changes over two decades. Atmospheric Environment 198 (2019) 335–350. <https://doi.org/10.1016/j.atmosenv.2018.10.051>

WSL 1990/92: Swiss National Forest Inventory (NFI), data extracts 30 May 1990 and 8 December 1992. Swiss Federal Institute for Forest, Snow and Landscape Research, Birmensdorf. <http://www.lfi.ch/index-en.php> [22.11.2018]

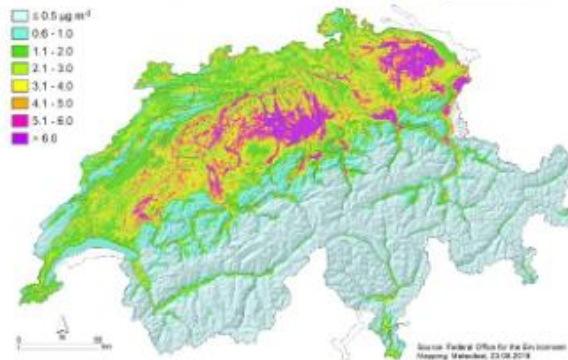
B Annex: Time series maps

The following overview maps are shown for the years 1990, 2000, 2005, 2010 and 2015:

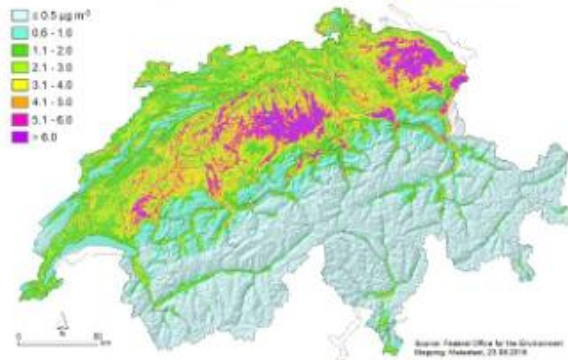
- Ammonia concentrations
- Total atmospheric nitrogen deposition
- Maximum exceedance of critical loads per raster cell (1x1 km²)



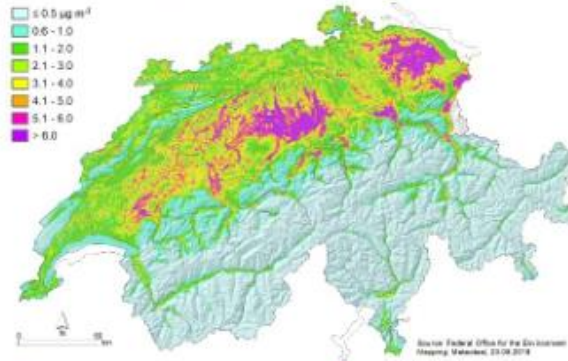
1990 Ammonia concentration



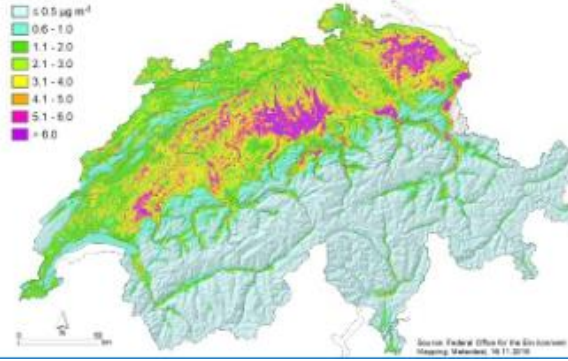
2000



2005

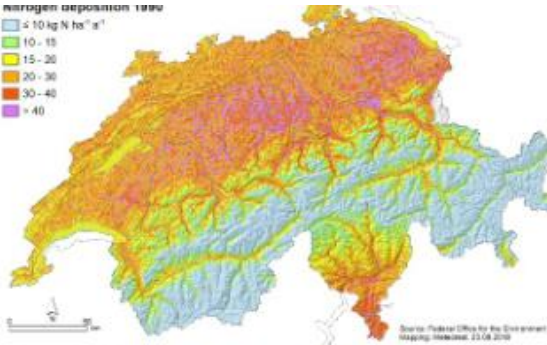


2010



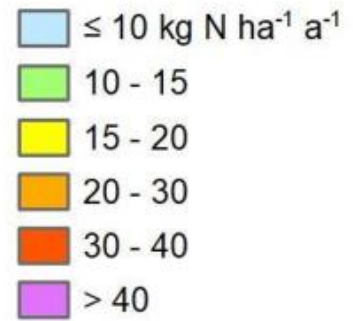
2015

Nitrogen deposition 1990



1990

Total deposition of nitrogen

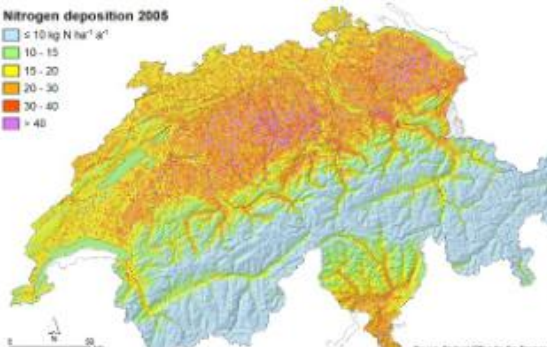


Nitrogen deposition 2000



2000

Nitrogen deposition 2005



2005

Nitrogen deposition 2010



2010

Nitrogen deposition 2015



2015



1990

Maximum exceedance per km²



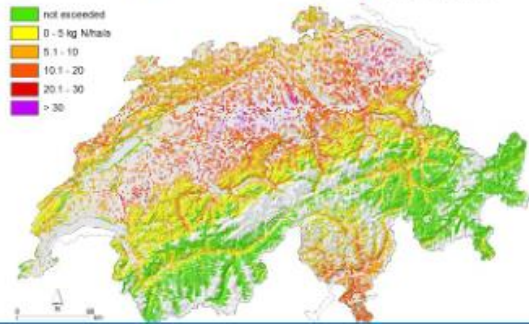
2000



2005



2010



2015